

Mapping the Most Energetic Cosmic Rays

A.M. Hillas

School of Physics and Astronomy, University of Leeds, Leeds LS2 9JT, UK

Abstract

The Pierre Auger Collaboration has shown that the cosmic rays detected to August 2007, with estimated energies above 57 EeV, were mostly very close to the direction of a catalogued AGN within ~ 75 Mpc. The closeness of the sources to us, and their association with the locality of moderate Seyfert galaxies rather than the most striking radio galaxies, were surprising, leading some authors to question the reality of the apparent associations. Here, three further techniques for examining the correlation of cosmic ray arrival directions with directions of AGNs are introduced to confirm and extend this correlation. These include the uniform-exposure polar plot to examine large-scale associations, and a sensitive “right ascension resonance” test to show the rapidity of the decoherence when the two patterns are displaced. The latter test avoids the choice of a correlation window radius, which makes it possible to see an AGN correlation in other data at a lower energy, and to seek it in HiRes data. On the basis of the closeness of correspondence of the cosmic ray and AGN maps, and the equally significant correspondence with directions of extended radio galaxies listed by Nagar and Matulich but not used in the Auger group’s investigation, it is argued that the association with these two sets of objects is by no means accidental, although the efficacy of the 57 EeV “cut” in selecting this revelatory sample may have been accidental.

The arrival directions of these cosmic rays (nominally close to 75 EeV) can be well described if most of the sources are in or around rather typical Seyfert galaxies, in clusters typically at ~ 50 Mpc, with the cosmic rays being scattered by $3 - 4^\circ$ on their way to us. Because of close clustering of AGNs, it cannot usually be ascertained which object within 2–3 Mpc is the actual source, but more than a third of the cosmic rays appear to come from FRI or similar radio galaxies in the clusters. It thus seems likely that these and also weaker jet-forming Seyfert galaxies are indeed causing acceleration to 10^{20} eV. Neither the brightest (nearby) radio galaxies nor the Virgo cluster dominate the cosmic-ray sky as had been expected, and Cen A is probably one of the currently inactive 10^{20} eV accelerators, as much more distant FRI galaxies play such a large role. The deflections cannot be much more than $3 - 4^\circ$ without destroying the coherence. Intergalactic magnetic fields ~ 1 nG could be responsible, but in one part of the sky a displaced “resonance” suggests a possible 4° deflection by the B_z component of our local Galactic magnetic field. A source region limited to <120 Mpc for the Auger cosmic rays is supported. This is compatible with a GZK survival horizon but only if (a) the sudden fall in the energy spectrum is not simply a GZK effect but essentially reflects the energy cut-off in the accelerators, and (b) the Auger energies are underestimated by $\sim 25\%$.

Key words: Cosmic ray origin, AGNs, Equi-exposure skymap

1. Introduction to the new observations of arrival directions of the most energetic cosmic rays

In 2007 the Pierre Auger Collaboration [1] published the directions of arrival of 27 cosmic-ray particles which they estimated to have energies above 5.7×10^{19} eV (57 EeV), and near most of these directions (within 3.2°) there was an active galactic nucleus (AGN) listed in the 12th Véron-Cetty Véron catalogue (abbreviated below as VCV) [3] within a distance of about 75 Mpc of Earth (if $H_o = 72 \text{ km s}^{-1}\text{Mpc}^{-1}$, as assumed below). The probability of such a close association appeared to be very small if the cosmic rays arrived from near-random directions as only 21% of cosmic rays would be expected to match so closely in this case. By contrast, many air shower experiments had previously sought evidence for the sources of cosmic rays above 10^{17} eV, but had failed to find any convincing departures from isotropy, supporting the belief that deflections of the particles in irregular magnetic fields had scrambled their directions of motion. Above about 60–80 EeV, though (depending on the maximum energy of particles leaving the

11 sources), few protons or light nuclei would reach us from beyond very few hundred Mpc because of energy losses
12 in the cosmic microwave background radiation (the GZK effect), and so the particles from far off, that would have
13 been highly deflected en route, should be absent. The Auger experiment in Argentina is unique in its huge collecting
14 aperture, its very uniform sensitivity to cosmic rays above 10^{19} eV (within 60° of the zenith), well-measured energies
15 in this context, and, apparently, an inspired unexpected choice of the VCV catalogue to check for significant patterns
16 in the arrival directions. The data set will be greatly expanded in the next few years, but it already shows that, firstly,
17 the most spectacular double-lobe radio galaxies that dominate the radio sky are not the principal suppliers of these
18 extreme cosmic rays, secondly, the expected beacon of the local skies, the Virgo cluster, is also relatively unimportant,
19 and in fact most of these extreme cosmic rays appear to originate in less remarkable Seyfert galaxies or else in sources
20 that cluster in their vicinities (say 2-3 Mpc). Looking outside the VCV catalogue of optically-detected AGNs used in
21 the Auger report, it is found additionally that a considerable minority of these cosmic rays correlate about as closely,
22 and perhaps even more significantly, with extended radio galaxies within the same distance range, although somewhat
23 further away than those which dominate the radio sky: a set of sources brought to our attention by Nagar and Matulich
24 [10]. Very fortunately, it seems that, at these energies, deflections of the particles over 100 Mpc are not more than
25 a few degrees. However, it will be proposed that this description applies only to the proton component of cosmic
26 rays, whereas there is evidence that above 40 EeV most particles are highly charged; so a detector's bias in favour of
27 protons may strongly influence the pattern that it sees.

28 It is a novel feature for charged-particle astronomy to reveal a rich pattern of point sources, and these surprises have
29 led to challenges. It is the first main object of this paper to provide further methods of analysis that greatly strengthen
30 the evidence that these details of the arrival patterns are real, and then to examine the most probable implications
31 regarding the origin, nature and energies of the particles, that can be straightforwardly tested with more data.

32 The unexpectedness of these reported correlations led commentators to express doubts of many kinds. First,
33 regarding the methodology, it has been suspected that the apparent statistical significance of the result has been
34 artificially generated by the use of the first half of the Auger observational data set to vary the selection "cuts" in
35 energy threshold (57 EeV), maximum redshift of catalogued AGNs to be used in the correlation (< 0.018), and the
36 correlation window size (3.2°): all chosen to maximize the significance of the departure from isotropy in this first
37 subset. Several early discussions of the arrival directions have put aside the apparent close correlation with weak
38 AGNs, and considered large magnetic displacements from the directions of expected strong sources [4, 5, 6]. The
39 use of the VCV catalogue based on optical appearance of galaxies, rather than one with more emphasis on high jet
40 luminosity indicated by strong radio or X-ray emission, has been questioned [7, 8]. Different proportions of AGNs
41 will be included in the catalogue in different regions of space. A deduction that most of the sources are less than 100
42 Mpc away has been remarked on as strange [12]. The northern-hemisphere HiRes experiment found no association
43 of the most energetic cosmic rays with AGNs [13]. The very weak level of activity of some of the AGNs picked out
44 in the study has been remarked on as making their identification as cosmic-ray sources implausible. (It should be
45 pointed out that the Auger authors did not claim to discriminate between the AGNs or other objects that reside in the
46 same localities as the AGNs. Their published study was intended to demonstrate anisotropy rather than to explain it
47 at this stage.)

48 Whilst the aim of the research is to understand how particles are accelerated to these extreme energies [4, 5, 12],
49 the emphasis in this paper is on extracting as clearly as possible the simplest pointers to sources that are present in
50 the cosmic-ray directional data, largely avoiding scrutiny of particular accelerators. When three times the presently
51 published data set is available, it should be possible to pay attention to individual sources. So it is the purpose in this
52 paper to tackle many of these doubts, and to show that the evidence can be extended. The clumpy pattern on the sky of
53 these AGNs can be demonstrated by a simple extension of the Auger "window" counts, and this clumpy distributions
54 of cosmic rays and AGNs on the sky can be better visualised and quantified by an alternative form of mapping, using a
55 uniform-exposure polar plot. A simple model of apparent origins of cosmic rays scattered around VCV AGN locations
56 describes also the overall pattern of the cosmic rays. (The clumping also implies that not all AGNs near the cosmic-
57 ray line of sight are necessarily the relevant sources, so several objects can have been misidentified as sources.) A
58 "right ascension resonance" test is introduced as a striking and sensitive demonstration of the association with AGN
59 localities, using which such associations can later be sought using a different list of potential sources, in data of other
60 experiments, and potentially at other energies, and a hint of magnetic deflection appears.

61 The work is laid out as follows. The direct evidence of the density and clustering of AGNs near cosmic-ray
62 directions is examined in section 2, showing that the particles do not come precisely from the AGNs, but are distributed

63 within $\sim 3 - 4^\circ$. In section 3, the use of the uniform-exposure polar plot is introduced, to show where these clusters
64 are on the sky, and demonstrating first the anisotropy of the cosmic-ray distribution without regard to AGNs, and then
65 that its large-scale features do match those of the AGNs in the VCV catalogue (which has a “useful” distance bias),
66 apart from a possible anomaly in the direction of the Virgo cluster, which will be re-visited later. Section 4 introduces
67 a “right ascension resonance” as an alternative to the Auger method of detecting a correlation of cosmic ray directions
68 with AGNs, but not requiring the choice of a particular “window radius” for counting nearby AGNs, and avoiding
69 the large statistical penalty which the choice of this radius involves. Using this, an AGN association can be sought in
70 the results of two experiments viewing the northern hemisphere. In section 5, the correlation of cosmic rays with an
71 alternative set of AGNs, “extended radio galaxies” [10], will be considered. In section 6 the resonance technique is
72 used to seek evidence of magnetic deflections where particles arrive after following a long path just above the disc of
73 our galaxy. Section 7 explores the extent in redshift of the AGN correlation, finding rough agreement with the Auger
74 group’s conclusion that most of the particles reaching us at these energies have travelled less than 100 Mpc. In section
75 8, it is argued that this implies an underestimation of particle energies, and also implies that the reported steep fall in
76 the cosmic-ray spectrum is not simply a “GZK spectrum cutoff”, but largely a downturn of the energy spectrum of the
77 accelerators, which imposes a “GZK distance horizon”; but the details are sensitive to probable energy measurement
78 errors. Some principal conclusions are summarized in section 9.

79 Appendix A introduces some relevant shortcomings of the VCV catalogue of optically-detected AGNs, which
80 limit the range of source distance for which this catalogue can be used. Figure 13 in the appendix shows the number
81 of objects visible from the southern hemisphere that are listed per Mpc of distance and in different ranges of absolute
82 magnitude, which indicates that the completeness of the catalogue for fainter objects (some of which may nevertheless
83 be particle accelerators) is continually decreasing with increasing distance, and that beyond about 75 Mpc the gaps
84 may be serious, so that it will be more difficult to use the VCV catalogue to explore further into space (as remarked in
85 [1]). If the number of listed AGNs per square degree had been much greater, however, the probability of associations
86 within 3.2° with any arbitrary direction would have been large, nullifying the signal. A sparser but uniform catalogue
87 would be better for such an exploration, and it will be seen that a catalogue of FRI radio galaxies may serve well
88 here. Indeed following up the suggestion of Nagar and Matulich [10], the correlation with such objects already adds
89 substantially to the significance of these associations.

90 2. Clustering of the AGNs: the cosmic ray source is often not the closest AGN

91 The evidence that these most energetic cosmic rays originate in the locality of AGNs was that, excluding 6 cosmic
92 rays arriving within 12° of the galactic plane, where most AGNs would be obscured by dust, and where cosmic rays
93 might be more strongly deflected by galactic magnetic fields, only 2 of the remaining 21 cosmic ray directions did not
94 have an AGN (redshift < 0.018) within an angular radius of 3.2° , whereas if one places such 3.2° windows at arbitrary
95 positions on the sky, governed only by the total exposure of the detector array to each region (but avoiding the vicinity
96 of the galactic plane), one finds only 24% of them contain AGNs.¹ (The average *number* of AGNs per window is
97 0.36.)

98 Though the statistics seem, and are, significant, such figures can always be enhanced by the selective choice of
99 examples to count; and the cuts in the data — the choice of 57 EeV as the energy threshold, of a redshift range below
100 0.018 and a window radius of 3.2° in which to count AGNs — were selected only when half of the cosmic rays had
101 been recorded (14 of the 27 events), in such a way as to maximize the significance of the departure from randomness,
102 these cuts being fixed thereafter, in order to confirm the anisotropy — though actually slightly modified later (3.1
103 became 3.2, 56 became 57). There is no physical reason for expecting 3.2° to be appropriate: this value may serve
104 mainly to minimize the chance of random unassociated AGNs being counted. This optimization of the cuts using half
105 the data must have enhanced the apparent association of AGNs: in the first half all 10/10 of the cosmic rays outside
106 the galactic zone had an AGN in their window: in the last half the proportion was 9/11. The bias is actually not huge,
107 but it is important to investigate it. Also, the next paragraph will supply support for the supposition that the galactic
108 belt should be excluded.

¹Note that the proportion 21% quoted by the Auger authors applies if the galactic obscuration zone is not excluded from the counts.

109 The low average density of 0.36 AGNs (in this catalogue and in this redshift range) per 3.2° window might be
 110 thought to indicate that when an AGN is seen in the window it must probably be the source of the cosmic ray particle,
 111 but this is not so, firstly because the AGNs are strongly clustered. The average number of AGNs per window drawn
 112 around the 21 selected cosmic rays (“window 1”, below) is 1.1, but the average numbers in the 3 surrounding annuli
 113 $3.2^\circ - 4.53^\circ$, $4.53^\circ - 5.54^\circ$ and $5.54^\circ - 6.40^\circ$ (“windows 2 to 4”, below), all of equal solid angle, are given in line (A)
 114 of the table 1.

window number	1	2	3	4
(A) $\langle N_{\text{AGN}} \rangle$ in windows around CR	1.1	1.1	1.0	0.7
(B) $\langle N_{\text{otherAGN}} \rangle$ around selected AGN	1.2	0.9	0.9	0.8

Table 1: Numbers of AGNs in concentric annuli.

115 Line (A) shows that there is typically a high local density of AGNs which extends for several more degrees. To
 116 find the typical density of AGNs in any region inhabited by AGNs, one can draw windows and surrounding annuli
 117 around any AGN, and line (B) of the table shows the average number of other AGNs found in these windows (the
 118 average being weighted by the array exposure at that declination, and avoiding the zone of low galactic latitude). The
 119 AGN densities around cosmic ray directions are little different: clearly an “other AGN”, unrelated to any that might be
 120 the cosmic ray source, is very likely to be found in the central window; so the AGN seen in the standard 3.2° window
 121 used by Auger may often be a neighbour unrelated to the cosmic ray. Indeed, if the cosmic rays always pointed back
 122 very close to a source AGN (always well within 3.2°), one would expect the numbers in line (A) to be like those in
 123 line (B) except for an additional 1 in the central window (because we are now counting the “central” AGN in addition
 124 to the “other” AGNs that were counted in line (B)), and the count in windows 1 and 2 of line (A) would be expected
 125 to differ by about 1.0, which they do not. A precaution is needed before carrying this arithmetic further, because the
 126 counts in the central window (window 1 in the above table) will be biased in the first half of the data sample, which
 127 was used to optimize the data cuts. (A sign of this selection bias in the first half of the data is that the average number
 128 of AGNs per window is 1.1 but there are no zeros — a quite un-poissonian distribution!) Using the second half of
 129 the data, with only 11 showers outside the zone of low galactic latitude, the numbers of AGNs seen, this time in
 130 successive ranges of 2.5° from the cosmic ray direction, have been counted, and are shown below in the line “OBS”,
 131 their numbers expressed as density per 9.80×10^{-3} steradian, this being the area of the standard 3.2° window. The
 132 excess number of counts at the closest distances is sensitive to how far cosmic rays are spread around a “source” AGN
 133 (either by magnetic scattering or by the size of a cloud of supposed accelerators such as magnetars or hypernovae).
 134 One can simulate the numbers of AGNs that would be found at different distances from a cosmic-ray direction if
 135 they are typically spread with r.m.s. distance 3.2° , 4° or 5° , for example, around AGNs chosen randomly from the
 136 catalogue, but then accepted with a probability matching the observational exposure to that declination. (One can only
 137 take a very simple approach in such a small sample, and the question of whether an AGN closer to us should have
 138 been given a higher weight will be taken up later.) The results are shown in table 2 as “SIM 3.2° spread”, “SIM 4.0° ”
 139 and “SIM 5.0° ”. Of several examples calculated, the r.m.s. spread of 4° gave the nearest match to the observations,
 140 though the scanty statistics do not offer much precision (but a spread in accordance with this will be estimated in other
 141 ways later).

angular distance ($^\circ$)	0	2.5	5	7.5	10	12.5	15
OBS	1.49	0.89	0.78	0.60	0.53	0.46	
SIM 3.2° spread	1.75	1.13	0.79	0.65	0.58	0.54	
SIM 4.0° spread	1.48	1.11	0.82	0.66	0.58	0.54	
SIM 5.0° spread	1.24	1.05	0.83	0.68	0.60	0.54	

Table 2: Surface density of AGNs near cosmic ray directions.

142 The observations thus suggest that cosmic-ray arrival directions have an r.m.s. spread of about 4° around typical
 143 AGNs, although this cannot be a universal constant as the AGNs will of course be at different distances. The AGN
 144 density remains considerably above the average density of 0.36 for $\sim 10^\circ$, indicating the typical extent of AGN

145 clusters.

146 Thus the cosmic rays may suffer magnetic scattering of 4° while travelling to the observer from an AGN source.
147 Since this is somewhat greater than the 3.2° radius of the Auger selection window, one should not place too much
148 emphasis on the type of AGN found closest to the cosmic ray or even in the window. The true source may well
149 lie outside the window; and *a prime reason why some AGN is almost always seen in the window is because they*
150 *are so crowded in the region around the source.* The appearance of particularly feeble objects in the list need not
151 cause surprise. Thus Zaw, Farrar and Greene [11] noted that whilst most objects picked out by these windows were
152 AGNs with bolometric luminosities above 0.5×10^{43} erg s $^{-1}$, two other neighbouring objects had been misidentified
153 as AGNs. It is found that a very strong association with cosmic rays still persists if only radio-detected AGNs are
154 retained in the catalogue (about 75% of all those listed). One probably has a mixture of galaxy types close by in
155 typical clusters, and one can deduce only that the sources lie in or near AGNs of a type that is very common in such
156 clusters — say comprising 1/3 or more of the population. But the evidence so far does not prove that AGNs are
157 sources. Since unusual activity in galactic nuclei, and growth of supermassive black holes, is believed to arise from
158 collisions between galaxies in clusters, it is also possible that the AGNs are not the sources but are serving as markers
159 of regions where other types of activity related to star formation are also concentrated. The role of AGNs as markers
160 of concentrations of general galactic activity has been taken up by Ghisellini et al. [16], who showed that clusters of
161 galaxies did indeed correlate with Auger cosmic ray directions.

162 Much of the following discussion will avoid the choice of a “window” of a particular radius, but before moving on
163 it is worth mentioning that, of the windows around the 6 cosmic rays in the galactic exclusion zone, somewhat crudely
164 set at a uniform belt within 12° of the galactic plane, only 1 contains a VCV AGN and the first two surrounding annuli
165 contain only 1 AGN in all (12 annuli). These do appear to be regions almost devoid of visible AGNs, supporting their
166 designation as obscured regions where we do not know the positions of AGNs, as this catalogue is based on optical
167 surveys, so tests of association cannot be performed (though the bright radio source Cen B does shine through the dust
168 and coincides with a cosmic ray).

169 Where are these AGN clusters? The large scale features of the cosmic ray directions and associated AGNs will be
170 examined in the next section.

171 3. Mapping the sky on a uniform-exposure polar plot

172 The Aitoff sky projection that is commonly used to show how cosmic-ray arrival directions relate to large-scale
173 astronomical features can illustrate the relationship between clear-cut structures, but is less suited to these irregular
174 and clumpy patterns. Not only does the varying efficiency of detecting cosmic rays in different parts of the diagram
175 disguise real variations in intensity, but adjacent regions are cut apart, and important great circles such as the galactic
176 plane twist sharply, making it hard to see whether the cosmic ray patterns relate to these planes. The pattern of cosmic
177 ray arrival directions is revealed much better in a uniform-exposure polar plot, described below, if one is content to
178 display one hemisphere, or slightly more, rather than the whole sky.

179 Although I first used this plot in the 1970s in correspondence about the Yakutsk observations, it was not fruitful
180 then, as no patterns emerged, and I regret not having published it, although it has been used a few times in publications
181 by colleagues (e.g. [18]). Only now, with many particles detectable above the GZK barrier, is a study of tens, rather
182 than thousands of arrival directions of great interest again.

183 Figure 1 shows such a plot, for the 27 Auger cosmic rays. The plots are always centred on a pole — the south
184 celestial pole in this case. If δ is the declination of a point in the sky, and p its polar distance, ($p = 90^\circ - \delta$ for a
185 north polar plot or $p = 90^\circ + \delta$ for a southern plot), the radial coordinate, R , in the plot, representing polar distance, is
186 non-linear, being adjusted according to the total exposure of the observatory to each band of declination, so that the
187 area of any band of p is proportional to the number of particles that would be detected in that band if the particles
188 arrived at the earth isotropically. Particles detected from an isotropic flux would then yield a plot with a uniform
189 density of points per unit area, apart from the usual accidental statistical fluctuations.

If, for an isotropic flux, one detects $n_p(p)$ particles at polar distances less than p , out of a total of n detected
particles,

$$R = \sqrt{(n_p/n)} \quad (1)$$

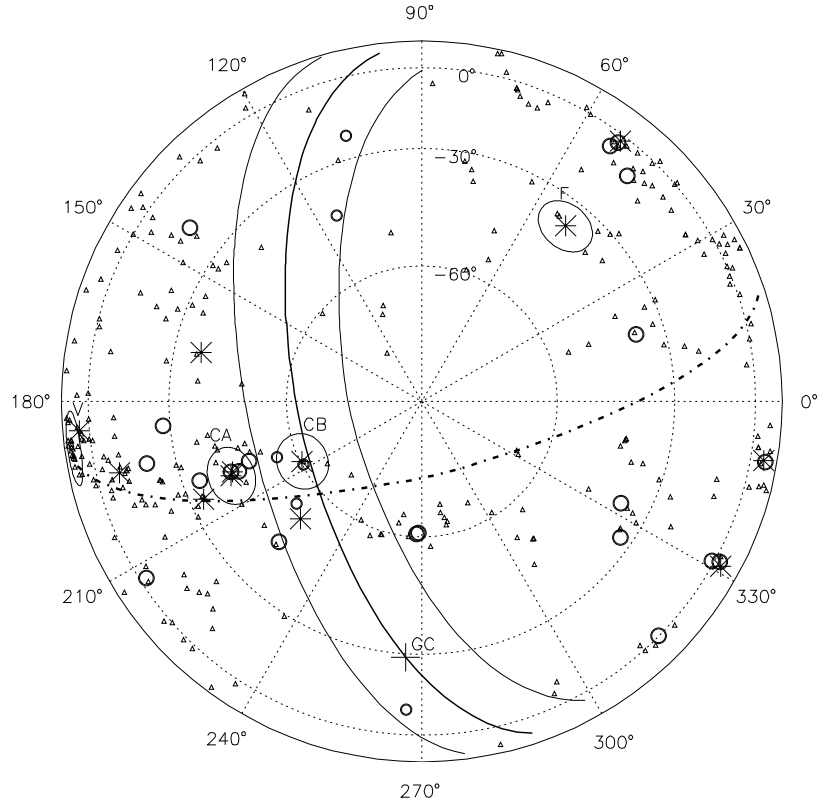


Figure 1: The 27 arrival directions of particles above 5.7×10^{19} eV, published by Abraham et al. [1] on a uniform-exposure polar plot. The 6 particles within 12° of the galactic plane are shown as smaller circles. NB: near R.A. 268° , dec. -61° there are two cosmic rays extremely close together. The galactic plane and circles of galactic latitude $\pm 12^\circ$ are shown as full lines (GC marking the galactic centre) and the supergalactic plane as a dot-dash curve. Declination circles at 30° intervals, and radial right ascension lines, are shown dotted. Circles of 6° radius drawn around some of the strongest radio galaxies – V, Virgo A (M87), CA, Cen A, CB, Cen B and F, Fornax A – illustrate the compression of the radial scale towards the edge. (A 6° circle represents the angular distance from a source within which (at ~ 40 Mpc) most of these cosmic rays arrive according to the analyses discussed here.) Virgo A is at the centre of the Virgo cluster of galaxies. Small triangles mark the positions of 280 VCV AGNs S of declination $+18^\circ$, having redshifts < 0.018 . Eight-armed crosses (stars) mark the extended radio galaxies listed in [10].

190 (The diagram has unit radius.) The azimuthal angle $\phi = \alpha$, the right ascension. A comment is appropriate here for
 191 the armchair astronomer. With this choice of α (increasing anticlockwise), this diagram looks very much like a true
 192 spherical sky globe seen from within in the case of the southern sky (and so represents the sky much as it really looks):
 193 but a northern hemisphere plot would look much like a sky globe viewed from the outside (giving a left-to-right mirror
 194 image of the constellations). In the north, this physicist's convention for plotting right ascension can be disconcerting
 195 to those astronomers who actually look at the sky, but will have the advantage of allowing the viewer to follow features
 196 such as the Virgo supercluster continuously from one hemisphere to the other.

197 If the observatory can record cosmic rays arriving at any point on a well-defined ground area, A , independent of
 198 their zenith angle of arrival, θ , out to a maximum zenith angle θ_{max} — as is the case for the Pierre Auger Observatory
 199 at energies above 10^{19} eV, where $\theta_{max} = 60^\circ$ — the detection efficiency at each declination or polar distance is well
 200 defined and the radial scale $R(p)$ in equation 1 can be derived from first principles. For the Auger case, with $\theta_{max} = 60^\circ$
 201 and latitude -35.2° , the radius R is tabulated in appendix B, table 4; alternatively an approximate formula can be used,
 202 such as equation (5) in the appendix, which has a maximum error of 0.006. Polar angles appreciably beyond 114°
 203 are unobservable — and off the diagram. In other cases, one would generally use data on the relative numbers n_p/n
 204 of detected particles in some well-defined lower energy band, close enough to 57 EeV (or whatever) for the detecting
 205 conditions to be virtually the same, but low enough for the particles to be approximately isotropic and much more

206 numerous. Substitution of these numbers in equation 1 gives the radial scale $R(p)$ for the plot.

207 Even without considering a connection with AGNs, the 27 Auger showers shown in figure 1 appear to be dis-
 208 tributed non-randomly, but the eye and brain will usually imagine an interesting relationship in a pattern of dots
 209 (“canals on Mars”). To characterize the clumpiness of the pattern of points, the cumulative distribution of the 351
 210 inter-point distances Δ as measured on the plot is shown in figure 2, and the average sky separation in degrees corre-
 211 sponding to the various separations Δ on the uniform-exposure plot are shown along the bottom of the graph.

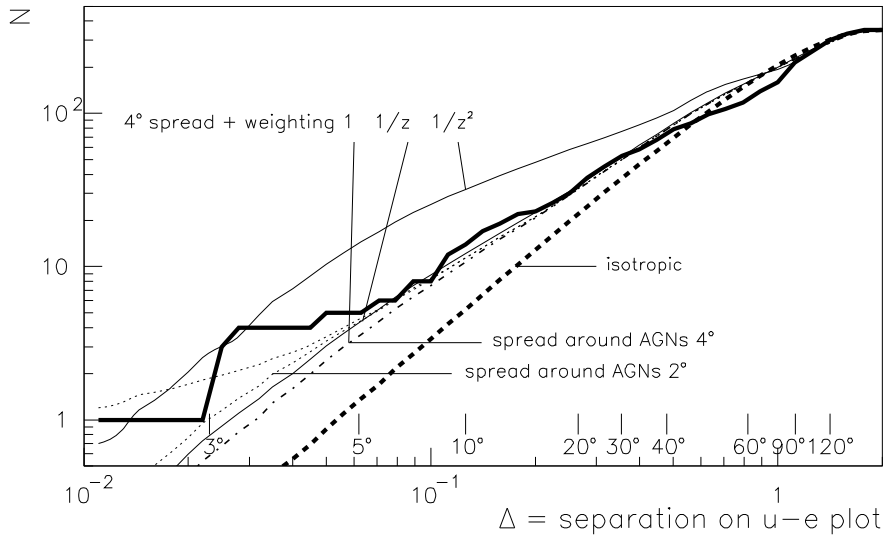


Figure 2: Cumulative number N of inter-point distances Δ on uniform-exposure plot in figure 1 for the 27 Auger cosmic-ray directions. The average separations in degrees on the sky, to which these plot-separations Δ refer, are shown just above the horizontal axis. Thick line: the observations (fig 1). Thick dashed line (“isotropic”), shows the average $N(\Delta)$ for many sets of 27 points placed randomly on the plot, simulating cosmic rays approaching the earth isotropically. Dot-dash line: average $N(\Delta)$ for many sets of 27 directions of AGNs picked from the VCV catalogue (redshifts $z < 0.018$) and given a 4° rms scatter (with refinements described in the text). Changing the scatter to 2° or 0.5° produces the variants shown by dotted lines. If a distance weighting is applied when picking AGNs, a $1/z^2$ weighting (appropriate if catalogue unbiased) moves the (4°) curve to the upper thin full line; the preferred $1/z$ weighting (see text) gives the full-line curve little different from the unweighted (dot-dash) version.

212 When compared with the inter-point distances found in a large number of sets of 27 points placed randomly on
 213 the circular plot, the cosmic rays show a large excess of separations at all angles below 30° , clearly non-random, as
 214 fewer than 1 in 400 of the random sets match the high number of inter-point distances in the range 10° - 14° , related
 215 to the size of clumps. The cosmic rays are thus clumpy quite apart from what AGNs tell us. (An analogous test
 216 for randomness was reported in the Auger paper [1], based on inter-event distances on the sky, rather than on an
 217 equal-exposure plot.) To test how well the AGN distribution as a whole accounts for this large-scale pattern, one
 218 can construct simulated sets of 27 cosmic ray directions by picking AGNs randomly from the catalogue, choosing a
 219 “cosmic ray direction” by applying a Gaussian displacement of rms angle 4° (Gaussian displacements of $4^\circ/\sqrt{2}$ in
 220 two perpendicular directions), and then accepting the direction with a probability given by the Auger array detection
 221 efficiency at that declination (table 4). There is a complication, as 20% of the sky is effectively occupied by the
 222 galactic zone in which many AGNs are hidden, so most of the cosmic rays within 12° of the galactic plane are not
 223 reproduced in such a simulation. It seems, in fact, not to change the inter-point distribution greatly, but to check this,
 224 a population of simulated cosmic rays has been generated by adding “infilled” fake AGNs in the galactic exclusion
 225 zone, by a process of copying random AGNs of rather similar supergalactic latitude and shifting them in supergalactic
 226 longitude into this zone. The distribution of inter-point distances for these simulated cosmic ray directions is shown
 227 by the dot-dashed line in Figure 2, and the effect of reducing the r.m.s. scatter about the AGN directions to 2° or 0.5°
 228 is shown by two dotted lines. They fit the observed distributions rather well except for a strange deficit, in real cosmic
 229 rays, of separations near 50° – low gradient of distribution — with an excess (steeper gradient) near 80° (separations

230 near 0.7 and 1.0 on the plot). There is also one exceptional small separation; and three more around 3° may lie outside
 231 the average distribution, but some of these could occur quite naturally. One of the latter is aligned with the very
 232 close AGN Cen A (3.4 Mpc), so if Cen A is the source, deflections could possibly be reduced in this case. Also, if
 233 these cosmic ray “deflections” represent magnetic scattering in a patchy magnetic field, the angle between a pair of
 234 arriving particles of similar energy from one source can be appreciably less than the typical overall deflection, so a
 235 simple model of independent deflections will underestimate the frequency of arrival of close pairs. (Apart from one
 236 unusually energetic event, the rms energy spread of the Auger particles is only 15%.) The overall pattern of cosmic
 237 rays on the sky thus supports the supposition of their emission from the localities of AGNs.

238 But this process of selecting randomly the AGNs to serve as source locations ignores the $1/z^2$ geometrical atten-
 239 uation of cosmic ray flux that should occur when deflections are small, favouring the AGNs closest to us, and also
 240 ignores an opposite correction for the incompleteness of the catalogue at greater distances. Regarding the latter point,
 241 in figure 13, the distance distribution of the most luminous objects, which would suffer least from a flux detection
 242 threshold, varies as $dn/dz \propto z$ at low z , as would happen in the case of matter distributed uniformly in a thin slab,
 243 though the angular spread of AGNs seen in figure 1 indicates that they spread much more widely than a slab configu-
 244 ration, so the real dn/dz distribution is probably tending towards a more isotropic z^2 variation at larger z . The overall
 245 trend of all catalogued AGNs in figure 13 is roughly $dn/dz \propto z^{0.3}$, so the numbers of catalogued AGNs may have
 246 to be multiplied by a factor in the range $z^{0.7}$ to $z^{1.7}$ to correct their apparent space density. When combined with the
 247 cosmic ray geometrical flux attenuation factor $1/z^2$ this suggests that the most reasonable distance-weighting factor
 248 for selecting “source AGNs” would be in the range $z^{-1.3}$ to $z^{-0.3}$. A distance-weighting factor $1/z$ is a reasonable
 249 compromise for the present (stopping the variation at $z < 0.001$ to avoid infinities), and the use of this factor made a
 250 slight improvement to the modelled curve in figure 2, shown by a full line slightly above the previous “model” curve
 251 (dot-dash). If the catalogue had been supposed equally complete at all distances, and the factor $1/z^2$ thus applied
 252 (down to $z = 0.001$), the very discordant higher curve is obtained, as a few extremely close sources dominate, very
 253 much at variance with the observations.

254 The Auger paper showed that where there are cosmic rays of such extreme energies there are AGNs nearby. Are
 255 there cosmic rays wherever there are AGNs (within 75 Mpc)? The overall clumpiness of the cosmic ray distribution
 256 has been shown to be consistent with this; different source regions are examined next.

257 Figure 3 divides the equal-exposure plot into 50 segments of equal area, a coarse resolution which seems appropri-
 258 ate for this situation. (Five annuli, of equal radial thickness, are subdivided into 2, 6, 10, 14 and 18 equal segments in
 259 right ascension.) To compare the distribution of detected cosmic rays with that of VCV AGNs (with redshifts < 0.018)
 260 as potential sources, in figure 3 each AGN was in version (a) simply given a weight proportional to the detection effi-
 261 ciency of cosmic rays from that direction, and the (rounded) total weighted number of VCV AGNs is printed in each
 262 segment, or in plot (b), a distance-dependent factor proportional to $1/z$ was also included in the weight, as suggested
 263 above. In both version (a) and (b), the weights were scaled to give 1 on average within a radius of 0.75 in the diagram.
 264 In the simple version (a) the weight was then 1.61 in the centre.

265 In order to compare cosmic ray and AGN patterns, only the 21 cosmic rays outside the $\pm 12^\circ$ galactic exclusion
 266 zone will be used: the cosmic rays clearly favour the segments containing many VCV AGNs. The numbers in (a) count
 267 AGNs when the only weighting is the exposure efficiency (version a), and in the 41 of these 50 segments that contain
 268 only 0 to 6 (weighted) AGNs, there are 101 of the 208 AGNs and 9 cosmic rays: the ratio CR/AGN is 0.09. In the
 269 whole diagram the ratio $CR/AGN = 21/208 = 0.10$. So even where AGNs are sparse, the proportion of cosmic rays is
 270 not lower than in the denser regions, suggesting in this small available sample that one does not need an exceptionally
 271 massive or rare AGN, such as is found at the centre of a large cluster, to supply cosmic rays. But the heavily-outlined
 272 Virgo segment has 26 weighted AGNs (representing a vastly greater actual unweighted number in the catalogue) and
 273 no cosmic rays, where one might expect about 2.6 (0.10×26). There may be a deficit here, although there is a 7%
 274 probability of recording no counts when 2.6 are expected. If the approximate distance-weighting factor (version b) is
 275 included, the overall features are not much changed. There are now 193 (weighted) AGNs, and 44 segments (those
 276 with AGN counts < 8) contain 102 of the 193 AGNs, with $CR/AGN = 0.12$ in these, and 0.11 overall. But here, the
 277 proximity of the Virgo cluster increases its weighting and one expects 3.8 cosmic rays from that segment, where none
 278 is observed, which does look anomalous. In each segment of the plot in figure 3, the weighted number of VCV AGNs
 279 is given, and also (smaller figures) their weighted average distance in Mpc. The important segments with more than
 280 6 weighted AGNs and at least one cosmic ray, in case (a) indicate 45 Mpc as the average distance — considerably
 281 further away than the Virgo cluster (at 16 Mpc) — whilst the smaller $1/z$ -weighted averages in case (b) indicate a wide

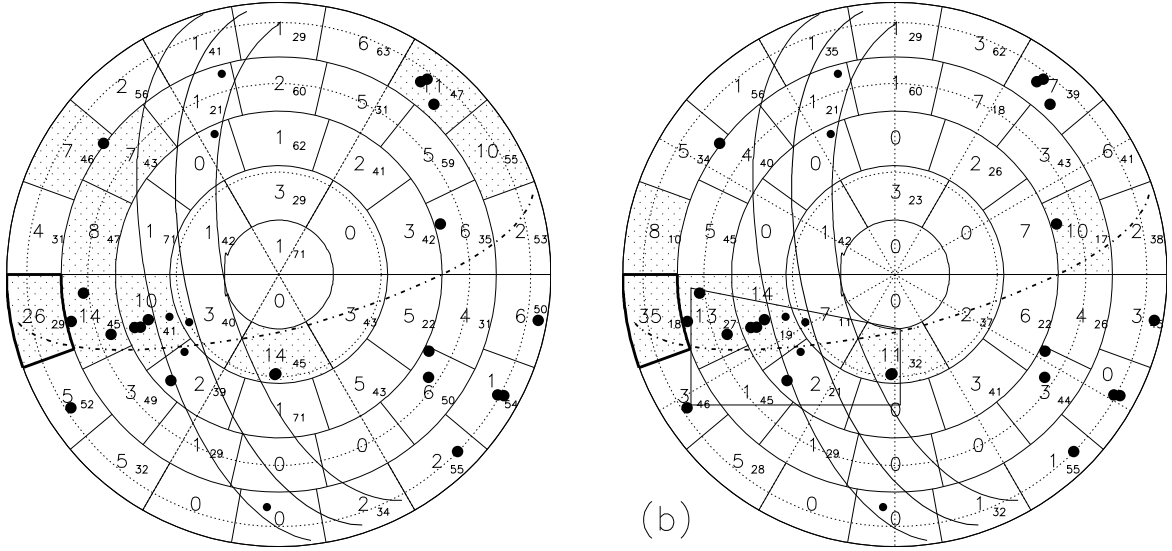


Figure 3: The uniform-exposure plot divided into 50 segments of equal area. (a) The larger numerals give the (rounded) number of VCV AGNs (at a redshift $z < 0.018$) in each segment, weighted by a relative array exposure factor (made to average 1 for radii < 0.75 , going to zero at the outer edge). Smaller numbers: weighted average distance of these AGNs, in Mpc. The 9 segments with weighted AGN count > 6 are shaded. (b) The same, but weight given to each AGN includes an additional factor $\propto 1/z$ (still normalized to 1): see text. Here the 6 segments with > 7 (weighted) AGNs are shaded.

282 spread in the distance of AGNs in these segments, though not necessarily in the distance of the dense active regions.
 283 Some cosmic rays may originate beyond the 75 Mpc limit of the sub-catalogue used here. Two of the 21 cosmic rays
 284 have no AGN within the standard Auger window of 3.2° . Is their source further than 75 Mpc, or is the displacement
 285 more than 3.2° ? A technique for extending the correlation radius will be proposed in section 4. A more sophisticated
 286 treatment of sensitivity of the catalogue at different distances would be appropriate when more data are available.

287 The most striking implication of these correlations is that cosmic rays must come from very many sources (many
 288 4° -spread circles being needed to cover the observations) within ~ 75 Mpc, and the most spectacular strong double-
 289 lobe radio galaxies do not supply a large part of them. Cen A supplies about $1/4$ of the total extragalactic radio-source
 290 flux at 1.4 GHz, with M87 (Virgo A) about $1/5$ of that, and Fornax A about $1/8$ of Cen A's radio intensity. Biermann
 291 et al. [5] expected these radio galaxies to dominate the cosmic ray flux if their jets are powered by the black hole
 292 spin, and suggested that intergalactic magnetic fields have displaced the cosmic rays from M87 very considerably,
 293 to give very many of the observed arrival directions along with the Cen A contribution (little displaced because of
 294 its proximity). A displacement of the Fornax A contribution was also proposed. However, if cosmic rays from M87
 295 (Virgo A) were to be redistributed over the region containing the observed cosmic rays in the lower left hand quadrant
 296 of figure 1, scattering points randomly over a quadrilateral shape containing these observed directions shown in outline
 297 in figure 3b, only 27% of the points outside the galactic exclusion zone would have a VCV AGN within 3.2° . The
 298 observed correlation with AGN positions is too close: such a large-scale deflection is not supported, within the present
 299 statistics. Gorbunov et al [6] similarly propose a large extension of Cen A cosmic rays, but evidence is given in the
 300 following sections that magnetic deflections are small. Moreover, Gorbunov et al. drew attention to the importance
 301 of the huge $1/z^2$ geometrical factor favouring Cen A because its distance is only 3.4 Mpc. This gives it an advantage
 302 of a factor ~ 200 compared with the typical VCV AGNs at 40-50 Mpc that appear to be correlated with cosmic rays,
 303 so Cen A should at least match all the others as a source of local cosmic rays. If it does not, we have to suppose
 304 that particle acceleration to the highest energies is discontinuous, and Cen A is in its off state so far as 10^{20} eV is
 305 concerned (the jet does not have a non-thermal hot-spot), and the same may be true of Fornax A. It has been noted
 306 that there are two cosmic ray directions within 3.2° of Cen A, but these might well come from another double-lobed

307 FRI radio galaxy, NGC 5090 (at 48 Mpc) in the list of Nagar and Matulich [10], and not in the VCV catalogue. This
 308 is within 1° of Cen A (see figure 1). The correlation of cosmic rays with these radio galaxies will be examined more
 309 quantitatively in section 5, but while figure 3 is before us, it can be seen that there are a close pair of cosmic rays
 310 near $\alpha = 341^\circ, \delta = 0^\circ$, in a very unremarkable segment of the diagram (1 or 0 weighted AGNs). The survey by
 311 Ghisellini et al. [16] also showed few normal galaxies here. There are not many AGNs in a further 50% of redshift
 312 either: is there a special object there? There is a BL Lac object with extended radio structure, PKS 2201+04, that
 313 Nagar and Matulich consider to be effectively an extended radio galaxy (see also [8]), though further away than the
 314 others, at 112 Mpc.

315 But why are no cosmic rays seen from the Virgo cluster region? Apart from any contribution from M87, the
 316 numerous other AGNs have as yet yielded no visible result, as remarked above. (a) Is it a technical problem of energy
 317 assignment or collection efficiency near the maximum zenith angle of 60° ? (b) Is the number of AGNs in the Virgo
 318 cluster exaggerated by the falling luminosity threshold for nearby AGNs in the catalogue, as referred to above? (c)
 319 Are the cosmic-ray sources not AGNs, but some other objects normally found near AGN but absent in the Virgo
 320 cluster? (d) Is cosmic-ray acceleration in Seyfert galaxies suppressed in a closely-packed environment? (e) Has the
 321 high density of gas generated a larger magnetic field in the supergalactic plane just here that deflects particles out of
 322 the plane (and out of our line of sight) and hides this source from us? Provisionally, it will be noted that option (b)
 323 is a distinct possibility, because, as noted above, the catalogue appears to have a bias crudely like a $1/distance$ to
 324 $1/distance^2$ effect. Such a progressive lowering of the power threshold at which AGNs are listed, as one moves to
 325 closer distances, may eventually move below the effective power threshold needed for cosmic ray generation, so that
 326 within some distance of Earth, many too-feeble AGNs are included in the catalogue. Zaw, Farrar and Greene [11]
 327 have favoured this explanation, noting that most Virgo cluster galaxies have bolometric luminosities below the values
 328 typical of other AGNs that correlate with Auger cosmic rays. A better view would be obtained from more northerly
 329 observatories, which provides an incentive to devise more sensitive tests for AGN association.

330 **4. A right ascension resonance: tracing the decoherence between the patterns of cosmic rays and of their** 331 **sources**

332 Is a 3.2° window the most suitable for seeking correlation between cosmic ray arrival directions and AGNs at
 333 different distances, in different parts of the sky, or at somewhat different energies? This is unlikely, whether this
 334 dimension arises from magnetic deflections or the size of galaxy or magnetar distributions, for example. Only the size
 335 and particular quality of the Auger data sample permitted a search for the optimal choice in their preliminary data set,
 336 and the best window size probably arose from its effect in reducing the confusion with background objects on the sky.
 337 For this reason, a correlation test that does not require a particular window size to be selected will be proposed, as an
 338 alternative technique for exploring the domain where this close association exists.

339 The notable feature of the cosmic ray directions in the original Auger report [1] was their angular closeness to
 340 AGNs. Hence a useful measure of association should be the angular distance, d_1 , between a cosmic-ray direction and
 341 the AGN nearest to that line of sight in a particular sub-set of the catalogue (such as a particular range of redshift).
 342 Here, d refers to the angular distance in degrees measured on the sky, and not to a distance on the uniform-exposure
 343 plot. Where $\langle d_1 \rangle$ is the average value of d_1 for a set of observed cosmic rays, let this be used as a measure of their
 344 association with AGNs. This should be significantly less than $\langle d_1 \rangle_{rand}$ evaluated for a set of the same number of
 345 pseudo-random directions. (Here, “pseudo”-random means that random directions are selected subject to weighting
 346 by the detector’s exposure to each part of the sky. They could be chosen using random points on the uniform-exposure
 347 plot, for example.) But what is “significant”? One would formally derive a probability, $P(\langle d_1 \rangle)$, that a random, or
 348 unrelated, set of directions would give such a low value of $\langle d_1 \rangle$, by simulating a very large number of “pseudo-random”
 349 sets, but it is hard to be sure that one has not inadvertently constrained the data in such a way as to produce a large
 350 error in $P(\langle d_1 \rangle)$, so such evaluations are always regarded with some degree of reservation. However, if the observed
 351 directions were put in the wrong position on the sky by a displacement $\Delta\alpha$ in every right-ascension angle, α , one
 352 would have a set of cosmic ray directions with the same detection efficiency, as this is independent of α . Figure 4
 353 shows the average distance $\langle d_1 \rangle$ to the nearest AGN when the relative right ascensions of the cosmic rays and the
 354 AGNs are shifted by $\Delta\alpha$ ranging from -180° to 180° . As just mentioned, for any value of the closeness measure $\langle d_1 \rangle$
 355 the probability that a set of 21 pseudo-random directions will have a value at least as small as this can be calculated
 356 by Monte-Carlo simulation, and the values of $\langle d_1 \rangle$ at which this probability has the magnitudes $10^{-1}, 10^{-2}, \dots, 10^{-7}$, are

357 marked on the diagram, by dotted lines. The cosmic rays which are (before shifting α) within 12° of the galactic plane
 358 have not been used, as for the vital small shifts $\Delta\alpha$ they cannot be usefully compared with the AGN map.

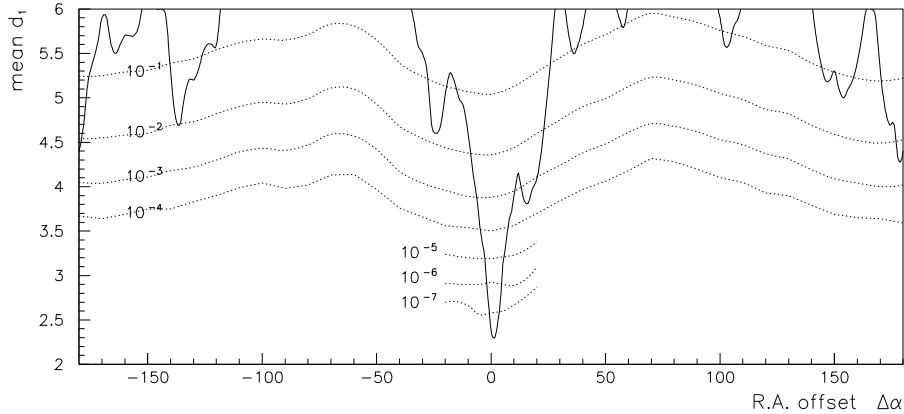


Figure 4: Right ascension resonance plot. Angular distance d_1 of cosmic ray direction from the nearest AGN ($z < 0.018$), averaged over the Auger set of 21 cosmic ray directions ($|b_{gal}| < 12^\circ$), plotted when the right ascension, α , of each AGN is shifted by $\Delta\alpha$. The near-horizontal dotted lines indicate the probability $P(\langle d_1 \rangle)$ of finding so small a value of $\langle d_1 \rangle$ in a set of 21 “pseudo-random” cosmic-ray directions at a specific offset position. (It varies with $\Delta\alpha$ because a 24° band almost devoid of AGNs is being shifted across the cosmic-ray pattern: only in the unshifted position does it coincide with the belt of omitted cosmic rays.) The preponderance of small distances d_1 soon disappears when the cosmic ray map and the AGN map are displaced slightly.

359 Only when $\Delta\alpha$ is close to zero is a clear association seen, with a chance probability $< 10^{-7}$ — a sharp “resonance”
 360 in right ascension. Not only is a low P seen, but one knows where it should appear. There is much noise, far from
 361 the resonance, as a few cosmic rays happen to pass accidentally close to AGNs, but the clumpy nature of the AGN
 362 pattern results in occasional surprising false correlations, such as is seen in the Auger pattern with a displacement
 363 near 180° . These off-centre troughs are not really significant, as the marked probability P refers to the chance of
 364 observing such a low value of $\langle d_1 \rangle$ at one particular $\Delta\alpha$, so if a randomly-positioned trough is typically about 6° wide
 365 near its tip, there are about 60 positions available for accidental troughs, and multiplying the marked probabilities by
 366 ~ 60 gives an indication of the chance of seeing so deep a trough by accident somewhere: one is very likely to see
 367 a purely accidental trough reaching a level of $P = 10^{-1.8}$. A trough within a very few degrees of the centre is expected,
 368 however, so the marked probabilities apply there.

369 There is a complication, because this rotation in α moves the galactic exclusion belt which contains very few
 370 AGNs across the pattern of observed cosmic rays. It is undesirable to reclassify the cosmic rays as in or out of the
 371 galactic exclusion zone, as changes the number of directions in the comparison, leading to several problems. For this
 372 reason, it has seemed preferable to move the AGNs, leaving the cosmic rays fixed, but this still leaves the empty belt
 373 moving with the shifted AGN distribution (so long as we use the optically-detected VCV AGNs), so, as the same set
 374 of 21 cosmic ray directions is used at all times, some of the “nearest distances”, d_1 , become appreciably larger for
 375 cosmic rays now falling in this belt. After testing several alternative remedies, the disturbance that this causes seems
 376 to be best treated by limiting all individual cosmic-ray d_1 values to a maximum or “capped” value of 10° . Not only
 377 does this suppress the main effect of having a nearly-empty belt, but it also prevents the existence of one or two cosmic
 378 rays 25° from any AGNs (their source perhaps being at higher redshift) from raising the overall $\langle d_1 \rangle$ by nearly a degree
 379 near the trough of the resonance. The movement of the empty belt of AGNs across the sky during this rotation causes
 380 changes in the probability of observing low values of $\langle d_1 \rangle$ by accident, as shown in the ups and downs of the dotted
 381 lines. Without the 10° cap, this variation is greater. In figure 4, $\langle d_1 \rangle$ at resonance is about 2.3° for the 21 cosmic rays
 382 in unobscured directions, whereas the average $\langle d_1 \rangle$ for pseudo-random sets of 21 is 6.8° , making the associated and
 383 unassociated populations well distinguished.

384 To estimate P at a particular shifted position, $\Delta\alpha$, of the AGN pattern, 100,000 “cosmic ray” points were selected
 385 randomly on a uniform-exposure plot, avoiding the 24° galactic exclusion zone, and the angular distance d_1 to the

386 nearest (shifted) AGN was recorded for each. Then, a set of 21 samples was drawn from these 100,000, and $\langle d_1 \rangle$
 387 calculated, up to 30 million such sets of 21 being produced, to find the frequency with which particular low values of
 388 $\langle d_1 \rangle$ were reached.

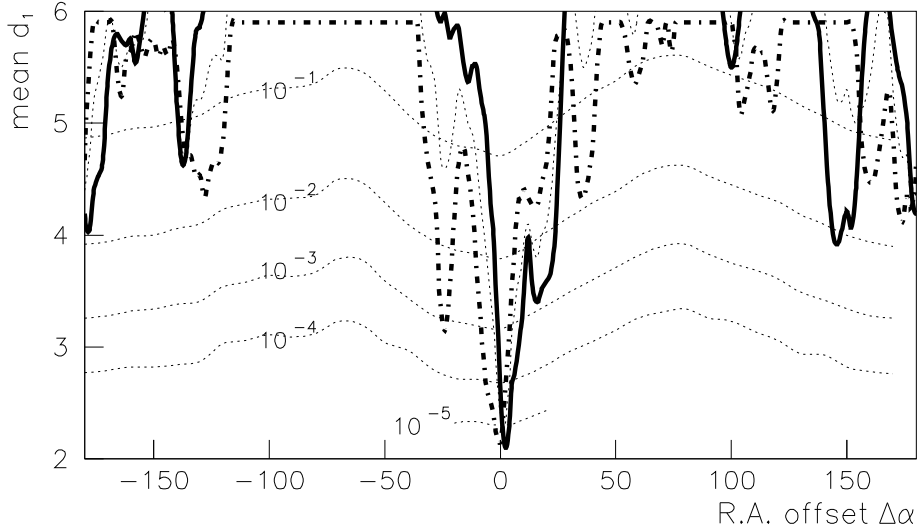


Figure 5: Right ascension resonance plot for subsets of the Auger data: (a) the first 10 cosmic rays $> 12^\circ$ from the galactic plane, used in choosing the selection cuts (thick dot-dash line), (b) the last 11 such cosmic rays, recorded after the cuts had been decided (thick solid line), and (c) all 21 such cosmic rays, repeated from figure 4 (thin dotted line). The dotted lines running across the diagram, showing the probability of reaching so low a value of $\langle d_1 \rangle$ at a specified $\Delta\alpha$, apply to the set of 11. See figure 4 for the probabilities applicable to a set of 21. The minima reached in subsets (a) and (b) have similar significance levels, in contrast to the probabilities of the numbers of 3.2° windows containing AGNs which was distorted in set (a) by the optimization process.

389 In the case of figure 4, the marked “probabilities” must be regarded with reserve, because the selection criteria
 390 for the data were decided half-way through the run, in such a way as to maximize the association as measured by
 391 the number of cosmic rays which had an AGN within a surrounding window of particular (optimized) radius. This
 392 $\langle d_1 \rangle$ resonance approach removes the relevance of window size, and this should remove the main source of bias,
 393 but the choice of maximum redshift for the test, and of energy threshold, might still influence the distribution in an
 394 accidental way in addition to the essential selection of the domain in which a real physical association exists. For this
 395 reason, figure 5 shows resonance plots for smaller data sets, one of which was taken after the selection cuts were fixed.
 396 The thick dot-dash curve refers to the 10 Auger showers from [1] outside the obscured zone of low galactic latitude
 397 that were observed before the selection cuts were chosen and which were used in making this choice; the thick full
 398 line applies to the 11 showers detected after this. The marked probability levels are for sets of 11 pseudo-random
 399 directions, and would be slightly different for the smaller first set. Even with only 11 observed directions, a 10^{-5}
 400 probability level is reached (and the same is true for 10). In the first data set all 10 of the standard 3.2° windows
 401 around the cosmic ray directions contained VCV AGNs (within 75 Mpc); in the second data set the hit rate was 9/11.
 402 The nominal probabilities for these hit rates are $10^{-6.1}$ and $10^{-3.5}$, but the first estimate is much too small because the
 403 selection cuts were chosen precisely to maximize this count, whereas selection of the cuts does not seem to have had
 404 such a distorting effect on $\langle d_1 \rangle$. The thinner dotted line shows the curve for all 21 events, transferred from figure 4. For
 405 the nominal probability values P that apply in this case, see figure 4: they are roughly the square of the probabilities
 406 shown for a set of 10 or 11 directions. At $\Delta\alpha$ near 145° one can see an accidental dip at around the depth in “ P ”
 407 ($10^{-1.8}$) that was suggested above as likely to occur, but there are some other dips, usually also not significant, that
 408 are related to the effect of clumps of cosmic rays being moved across a clumpy AGN field, as they recur in both
 409 sub-sets, and at $\Delta\alpha$ near -25° there is one that is probably partly random. The resonance technique could thus detect
 410 strong associations with AGN patterns in fairly small data sets, even when the best window size is not known. The

411 main conclusion from figure 5 is that the association between the cosmic rays reported in the Auger paper and the
412 VCV AGNs on a scale of a few degrees are very highly significant, and not generated accidentally by the optimization
413 process.

414 Four other applications of this right-ascension resonance will be considered. First: as the technique can reveal such
415 associations in data sets smaller than that of the Auger Observatory, do associations with AGN directions appear in
416 data of other experiments, viewing the northern hemisphere? This raises difficulties which are mentioned below, and
417 the real lessons to be learned are still being explored. Second: how significant are the associations with a different list
418 of target objects — the extended radio galaxies put forward by Nagar and Matulich? Third: can one detect systematic
419 displacements in the directions that could be caused by magnetic fields? Fourth: can one explore how far in redshift
420 the Auger association persists, to check the significance of the apparent 75 Mpc limit, and use the position of the GZK
421 horizon to check the energy of the particles?

422 As already remarked, the proportion of Auger cosmic rays to VCV AGNs appears to be lower than usual in the
423 region of the Virgo cluster, long assumed to be an important local source. The HiRes observatory was well placed to
424 observe this region, but reported seeing no cosmic ray excess in that direction, and indeed no association of cosmic
425 rays above 56 EeV with VCV AGNs, using the Auger windows. Would some other window size have been more
426 appropriate? Abassi et al. [13] estimated that the energies attributed by Auger to cosmic ray particles were too low by
427 10% (which is quite possibly an underestimate of the difference, as it depends on the energy at which a comparison
428 is made), compared with the HiRes scale, from a comparison of energy spectra, and so they picked out a sample of
429 cosmic rays for comparison having energies above (1.1×56) EeV on the HiRes scale. There were 13 HiRes events
430 supposedly above 56 EeV on the Auger scale [13, 14], and a resonance plot for the 10 outside the galactic obscuration
431 zone is shown in the upper panel of figure 6. The probability estimate is somewhat approximate, being based on the
432 declination distribution of stereo events above 10 EeV [15]. There is no signal at $\Delta\alpha = 0$, in conformity with their
433 paper [13] finding no correlations with AGNs. The single trough near -155° is a little unusual, though its probability
434 level is near that of the peculiar dip seen on the full-sample Auger plots near 180° , but with a different sample size.
435 (The events were displayed on a sky map in [13], but the positions used here were those tabulated on their web-site
436 [14], which seem to be consistent with the map.) If a uniform-exposure polar plot is made (as appropriate to the
437 HiRes observing conditions) there is no tendency for the cosmic rays to be less numerous in the segments which have
438 few (weighted) AGNs ($z < .018$), unlike what was seen in figure 3: the cosmic rays here do not follow the AGN
439 pattern even on a large scale. Is this astonishing disappearance of any AGN connection a feature of the northern
440 celestial hemisphere — or a surprisingly sharp change with energy that is not fully taken out by the 10% difference
441 assumed in the energy scales used in the two experiments? This has to be considered as there must be a rapid change
442 in Auger’s sky distribution just below 57 EeV because the optimization process found that the significance decreased
443 if the energy threshold was decreased despite a very rapid increase ($E^{-3.5}$ integral spectrum) in the number of events
444 available, but a list of Auger events below 57 EeV has not been published.

445 The much earlier experiment at Haverah Park pioneered the particle detector technique used at the Auger Ob-
446 servatory, and viewed the northern sky. Using the energy estimation methods then current, this experiment had 13
447 showers above 70 EeV, 11 of them outside the galactic exclusion zone ([19] with $\theta_{max} = 45^\circ$), and a resonance plot
448 for these cosmic rays, again matched against the VCV AGNs within 75 Mpc, is shown in the lower panel of figure
449 6. There is an apparent resonance with AGNs, with a 2% chance of being an accident. But the true energy threshold
450 of these Haverah Park cosmic rays cannot be 70 EeV because the exposure was only several percent of Auger’s: the
451 energy must be well below the 57 EeV at which the AGN correlation appears in the Auger observations, and thus
452 very many of these cosmic rays will originate beyond 75 Mpc, so the dip at 0° is less deep. An interesting feature is
453 that if 3.2° windows are drawn around the 11 shower directions, one of them contains 12 VCV AGNs (rather than the
454 typical 1.1), being aligned within 1° of M87 at the centre of the Virgo cluster, and if the AGN count is extended to
455 130 Mpc, another window contains 14 AGNs, being aligned within 3° of a cluster ($\alpha = 262^\circ, \delta = 58^\circ$) at 117 Mpc.
456 This suggests that the Virgo cluster is not completely inactive as a source, and disfavors the possibility that its output
457 is disguised by a large local magnetic deflection.

458 Investigation of the most reliable way to detect associations and estimate energy in such datasets is at an early
459 stage, and the result will be reported separately, but a comparison of these three experimental results suggests that
460 the 57 EeV threshold for association with nearby AGNs, found by Auger, may not be simply marking the point at
461 which interactions with the microwave background radiation limits proton survival to about 100 Mpc. The depth
462 of shower maximum measured by Auger [21] indicated that, unexpectedly, the particles become heavy, and hence

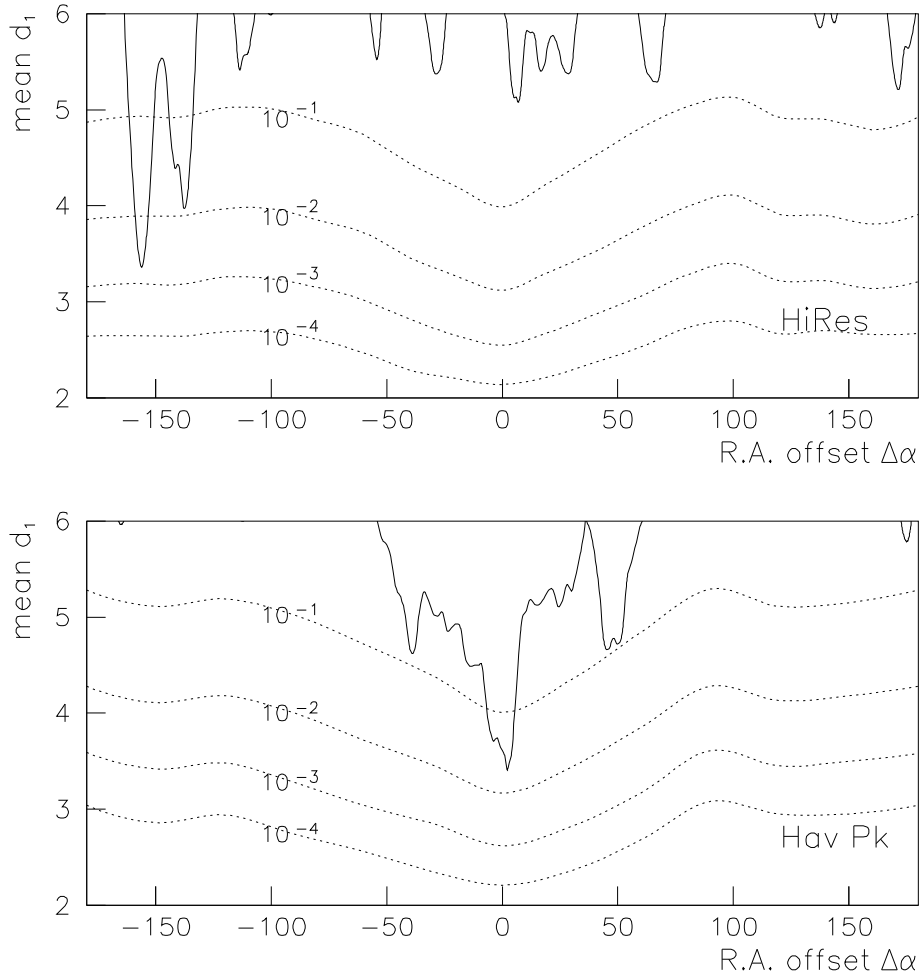


Figure 6: R.A. resonance plots for northern hemisphere observations: cosmic rays $> 12^\circ$ from galactic plane. Upper: HiRes: 11 cosmic rays estimated to have energies above 56 EeV on the Auger energy scale [13, 14]. Lower: Haverah Park: 11 cosmic rays originally estimated to have energies above 70 EeV, but possibly about half that.

463 highly charged and strongly deflected, as 50 EeV is approached, though not so below 30 EeV. This may be the only
 464 way to understand a wide spread of arrival directions in the HiRes data, if the fluorescence technique favours heavy
 465 nuclei rather more than does the array of water tanks (i.e. assigns them a slightly higher energy). The Haverah Park
 466 array did not find an expected GZK turn-down in the primary spectrum (as also AGASA, even more strikingly): the
 467 apparently most energetic particles were presumably the badly-measured ones that suffered large fluctuations in their
 468 energy assignment: and were probably thus protons. (The Haverah Park events also occurred in a somewhat lower
 469 energy domain, possibly before the highly-charged nuclei had become so important.) Why should these problems with
 470 energy assignment for individual proton showers not occur also in the Auger data? In that case, the domain above 57
 471 EeV apparent energy may be where an accidental tail of proton showers, which retain good directional information,
 472 emerges above the highly deflected component of heavy nuclei. The 57 EeV threshold would then be to a large extent
 473 an accident of technique (and an upper limit of the heavy nuclei), and the AGN signal might be highly dependent on
 474 shower selection. A method for rejecting heavy nuclei on the basis of the detector signals would be highly desirable.

475 **5. Correlations with extended radio galaxies**

476 There is a much smaller alternative catalogue, of large radio galaxies, against which the cosmic rays can be
 477 compared, which is equally significant, at the one-in-a-million level, may be virtually independent of selection-
 478 optimization bias, and is undoubtedly plausible, a priori. This is the set of 10 “extended radio galaxies” listed by
 479 Nagar and Matulich [10] as being within the declination range observable by Auger and the redshift range selected
 480 for the Auger analysis ($z < 0.018$). Nearly all are classified as probable FRI radio galaxies, except for Fornax A.
 481 These authors considered objects included in Liu and Wang’s [20] catalogue of galaxies with radio jets, and selected
 482 those for which the radio map showed emission whose total extension on the two sides added up to more than 180 kpc
 483 (scalar sum). Only three of these galaxies are on the VCV list of optically-detected AGNs — NGC 4261 (3C270),
 484 Cen A and Cen B, the latter being very near the galactic plane, although there is now no need to exclude the zone
 485 of low galactic latitude when comparing cosmic rays with radio galaxies, which shine through the dust. M87 does
 486 not meet their selection test. Concentrating first on the statistical argument, of 27 cosmic rays, 4 have at least one of
 487 these 10 radio galaxies within a “standard” 3.2° window; yet the average particle from an isotropic flux would have
 488 0.0015 such encounter by chance, and there is well below a 10^{-6} probability of having 4 “hits” in a sample of 27
 489 particles. As the selection conditions were not optimized for these targets, this appears to be an essentially indepen-
 490 dent demonstration that the cosmic rays are far from isotropic and truly associated with certain AGN-type objects
 491 (and the argument would be little affected if one removed the two galaxies that appeared in both lists and had nearby
 492 cosmic rays). The chance of having so many hits by accident is still under 1 in a million if directions are not chosen
 493 randomly but from a broad region of the sky corresponding to the cosmic-ray pattern in figure 1 but smeared out by
 494 30° rms spreading (in all cases the acceptance efficiency of the detector is taken into account). So the radio galaxies
 495 themselves do offer a pattern significance test essentially independent of the VCV association test. But a 3.2° window
 496 for counting associations is really too small for this situation in which the targets are less crowded on the sky, as will
 497 shortly be seen, so a $\langle d_1 \rangle$ resonance plot is shown, to check this level of significance, before moving on.

498 Figure 7(a) shows the mean distance in degrees of the 27 cosmic ray directions to the nearest of these 10 “extended
 499 radio galaxies”, as the right ascension of the objects is shifted, and plot (b) shows the same but in the next 50%
 500 extension of the redshift range (0.018 to 0.027), using the two further radio galaxies that Nagar and Matulich note, at
 501 positions ($\alpha = 52.7^\circ, \delta = -3.1^\circ$ on figure 1, 85 Mpc) and at 112 Mpc ($\alpha = 331.1^\circ, \delta = +4.7^\circ$). As these authors do not
 502 state whether there were any more similar galaxies in this range, there is some uncertainty about the full interpretation
 503 of this second plot, a subject that will be raised again when considering source distances in section 7. (Because the
 504 density of target galaxies is so low in this catalogue, the random separations are larger, and the angular distances d are
 505 capped at a value of 13° rather than 10° in forming the averages for these plots, though present results are insensitive
 506 to the precise value chosen.)

507 Without making a choice of window size, the significance of the association (case a) is not quite the same as
 508 quoted above using a “standard” size of window, but this is of no practical consequence.

509 These extended radio galaxies were selected from a list of galaxies with radio jets [20]. Are the other jets also
 510 effective sources? Omitting the (few) cases with short jets, with total length less than 1 kpc, the galaxies selected as
 511 having extended lobes comprise about 40% of the total in the localities considered here. A $\langle d_1 \rangle$ resonance curve for
 512 those that were not selected by Nagar and Matulich, shown dotted in figure 7a, shows no dip at $\Delta\alpha = 0^\circ$, indicating
 513 that they are not more strongly associated with cosmic rays than are the typical VCV AGNs.

514 It may be wondered how one finds room for more sources of these cosmic rays when almost all of them have been
 515 associated with optical AGNs, above. The explanation is, as remarked in section 2, that the close grouping of AGNs
 516 in clusters normally prevents identification of what object within a few degrees is the true source, which could be an
 517 object belonging to the cluster but not in the VCV catalogue. Most radio galaxies are such objects, and if they are
 518 indeed particularly efficient sources, we may in this case be able to identify the actual galaxy that is the source.

519 The usual 3.2° window size must be expected to exclude many cosmic rays if they do typically have rms spreads
 520 of $\sim 4^\circ$ around the VCV AGNs, and the counting window can safely be extended to 6° for greater counting efficiency
 521 when there is such a small density of targets on the sky: 4 more hits then appear, and there is no indication that one
 522 is picking up accidental pairings, although there may be a contamination from cosmic rays generated by other weaker
 523 sources in the surrounding cluster. In contrast with the VCV optically detected AGNs, which typically had ~ 0.1
 524 cosmic ray associated (see the discussion of figure 3), the ratio is close to 1.0 now: there are 12 cosmic rays that have
 525 at least one of these 12 extended radio galaxies within 6° (counting out somewhat beyond $z=0.018$ now), even though

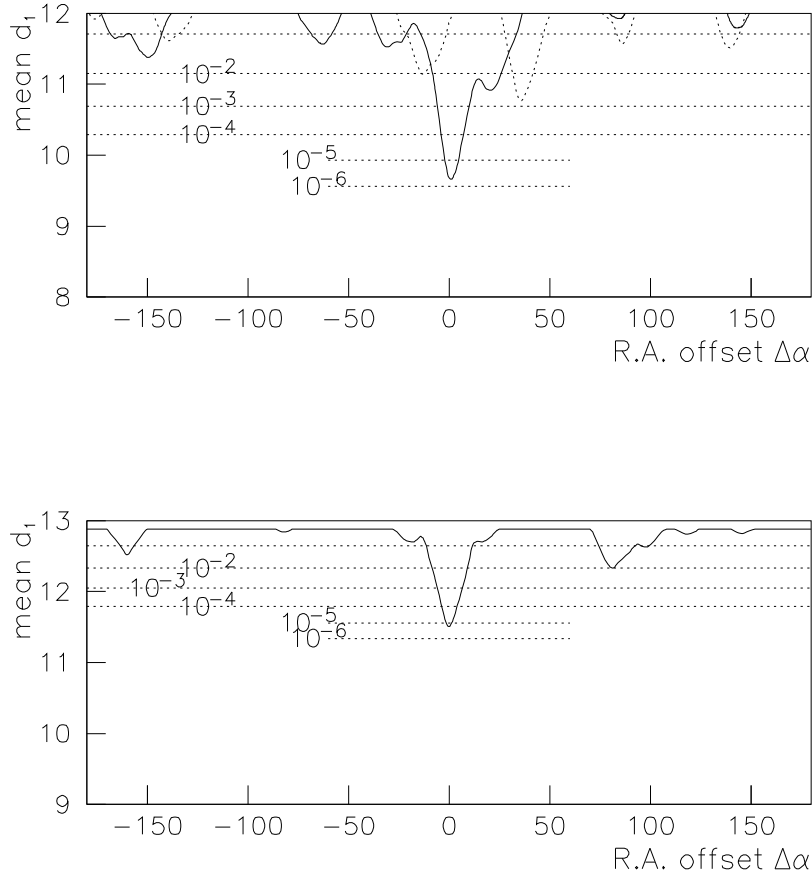


Figure 7: Association between the 27 Auger cosmic ray directions and the directions of extended radio galaxies listed by Nagar and Matulich. The mean distance between the cosmic ray and the the galaxy nearest on the sky is again measured in degrees. (a, upper panel) The 10 “extended” radio galaxies within 75 Mpc are considered; (b, lower panel) the listed radio galaxies (only 2) in the next 50% range of distance are used. The probability lines do not waver in level because there is no special galaxy avoidance zone moving across the sky now, for radio galaxies; but in case (b) the probabilities should not be relied upon, as the unbiased selection of the galaxies in this case is uncertain. (a) also shows, dotted, the resonance curve (but not the probabilities) for the radio-jet galaxies listed by Liu and Zhang that do not have extension greater than 180 kpc: they do not show a strong signal near 0° .

526 about 2 of these 12 cosmic rays could be attributed to surrounding VCV AGNs if they are contributing 0.1 each. Four
527 of these radio galaxies have no associated cosmic ray (Fornax A, 25 Mpc, NGC 3557, 43 Mpc, NGC 4261/3C270,
528 31 Mpc and NGC 4760, 66 Mpc), and it now seems likely that there is a fifth — Cen A. NGC 5090 (at 48 Mpc) has
529 three cosmic rays within 6° , and so has Cen A (3.4 Mpc) which is so nearly aligned that both these galaxies appear
530 in the same events. As Cen A has an advantage of ~ 200 in its $1/\text{distance}^2$ factor relative to most of the other typical
531 emitters considered here, but does not overwhelm them, it is probably in an “off” state, and the three cosmic rays
532 seemingly associated with it are then more logically attributed to NGC 5090. Other radio galaxies seem to have two
533 cosmic rays within 6° — Cen B (at 54 Mpc), Markarian 612 (83 Mpc) and CGCG 403-019/PKS 2201+04 (112 Mpc)
534 — though in some cases weaker sources in the cluster may perhaps contribute one. I am quoting the distances given
535 by Nagar and Matulich. As so many contribute more than one, the 5 undetected suggest that either the emission is not
536 continuous, or that the maximum energy is lower for some of them. The Nagar and Matulich galaxies should be seen

537 to associate with cosmic rays again in future Auger exposures.

538 In [10] it was proposed that these FRI galaxies were the essential sources, and that the remaining cosmic rays
 539 (perhaps 17 out of 27 from the figures above) were probably not really associated with VCV AGNs, and were ap-
 540 proximately isotropic. The authors also remarked that the correlation with VCV AGNs must be distorted by the
 541 inclusion in the catalogue of bright H2 galaxies that were originally mistaken for AGNs. Their suggestion has been
 542 tested by plotting a resonance curve for a reduced cosmic ray sample (having removed those which pass within 6° of
 543 Nagar-Matulich galaxies), and measuring their angular distances from the objects remaining in a reduced VCV AGN
 544 catalogue for $z < 0.018$ (having removed the 3 specified radio galaxies, and also the H2 galaxies as suggested). The
 545 result, plotted in Figure 8, shows that these cosmic rays that are not seen to be associated with the radio galaxies are
 546 not isotropic: there is still a pronounced trough close to 0° , with the chance that it arises by accident below 10^{-4} , still
 547 a very significant association.

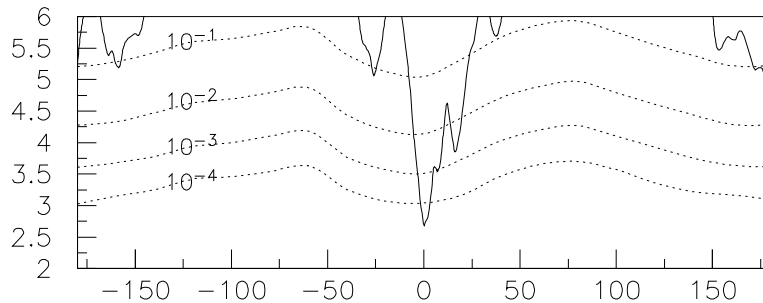


Figure 8: Figure 8. Plot of $\langle d_1 \rangle$ against R.A. shift $\Delta\alpha$ for cosmic rays which do not correlate within 6° with extended FRI radio galaxies (16 of the original 21 cosmic rays), compared with the positions of VCV AGNs after removing H2 galaxies (not true AGNs) and the extended radio galaxies from the list, to test a suggestion of residual isotropy by Nagar and Matulich [10]. The reduced set of cosmic rays still shows a strong association with the directions of optically detected AGNs.

548 One merit of the VCV AGN catalogue is that it contains the right density of objects to provide correlations with
 549 a large proportion of individual cosmic ray directions, but not so many as to make this correspondence unavoidable
 550 even with random directions, so it makes a striking demonstration of a close association with cosmic rays numerically
 551 possible if it exists. It has been argued above that this close association, very surprisingly, does exist, and is very
 552 significant even when allowance is made for the selection data cuts which optimized this correlation in the first half
 553 of the data-taking period. If one were to look to greater distances, however, source confusion would mount: there
 554 would be multiple close AGNs for many cosmic rays, confusing the picture quite apart from the need to allow for
 555 the opposite problem of serious catalogue incompleteness. The class of radio galaxy discussed above would be much
 556 more suitable than VCV AGNs to trace the extension of cosmic ray sources beyond 75 Mpc, because their number
 557 density is low enough to avoid source confusion, and the catalogue will not suffer from incompleteness until greater
 558 distances are reached. The X-ray selected AGNs in the Swift BAT catalogue can also be useful in this way, and George
 559 et al. [7] have already suggested that a correlation appears to extend to about 100 Mpc.

560 Thus it appears that both FRI radio galaxies and Seyfert galaxies can accelerate protons to 10^{20} eV, though the
 561 latter have a lower output. It seems that an intense hot-spot, as seen at the termination of FR II jets, and anticipated
 562 as a promising acceleration site [9, 5], is not implicated. If these two classes of active galaxy make up the relevant
 563 accelerators, the acceleration site may possibly be nearer to the base of the jet.

564 6. Magnetic deflections

565 If 3° of the spread of proton arrival directions around their sources represents a deflection in varying magnetic
566 fields in travelling ~ 45 Mpc, an effective transverse magnetic field $\approx 0.1\text{nG}$ would produce this. If the field changed
567 randomly on a scale of L Mpc, a typical total field strength in each domain of $\approx 1.6\text{nG}/\sqrt{L}$ would be required. This
568 must be an upper limit, as there will be other factors contributing to the scatter. A systematic deflection caused by a net
569 average field normal to the line of sight might be detected by a shift in the position of the “right ascension resonance”
570 from its expected position at $\Delta\alpha = 0$ — if the field had a component parallel to the earth’s rotation axis. But other
571 field directions can be investigated by shifting the AGN pattern in some other direction on the sky by choosing a
572 different axis for the pattern rotation. The resonance effect has been examined when the “AGN sky” is rotated through
573 small angles about the galactic pole or about an axis perpendicular to this (i.e. in the galactic plane, chosen to be at
574 a galactic longitude of 45° so as to be nearly perpendicular to the main concentration of cosmic-ray directions). Of
575 special interest is the set of AGNs at positive galactic latitude, seen on the left hand side of figure 1, for these 9 at
576 galactic latitude $> 12^\circ$ are mostly grouped in a small part of the sky and so may travel through a similar magnetic
577 field. On rotating the AGN sky about the special axis normal to the galactic pole, which is also about 90° from the
578 majority of these 9 directions, no perceptible shift from zero in the position of the resonance was seen (Figure 9c),
579 although this plot is very noisy, and a much larger data set may be needed to make clear what is happening. But
580 if a rotation about the galactic pole is made, thus shifting the AGNs parallel to the galactic plane, they are seen to
581 need an offset in order to match the cosmic-ray directions. To make the sampled region of sky more well defined,
582 two outlying cosmic rays may be omitted (one at much smaller galactic longitude than the others, and one at the high
583 latitude of 54°), leaving a more compact group of 7 arrival directions whose centroid is at galactic longitude 308°
584 and latitude 24° . The resonance curve (figure 9b) shows that the AGNs best match the cosmic ray directions when
585 offset by about 4° parallel to the galactic plane. (A shear was applied in these rotations, as described in the next
586 paragraph.) This sky rotation about the galactic pole tests any deflection of cosmic rays parallel to the galactic plane
587 (due to a “ B_z ” field component, perpendicular to the galactic disc), whilst the previously mentioned rotation tests any
588 displacement perpendicular to the galactic plane, due to a field component parallel to the plane (though cylindrical
589 symmetry of the galaxy may tend to make the averaged field along the line of sight nearly cancel out in this case,
590 where no displacement effect was found). No clear offset was seen if the other 12 (negative latitude) cosmic rays were
591 used (figure 9a). These directions are more widely scattered, and typically further from the galactic plane, where the
592 average galactic field strength might be considerably smaller.

593 A rotation of the AGN pattern about any axis, such as the galactic polar axis, produces a smaller actual displace-
594 ment on the sky as the pole is approached. Since the actual displacement of cosmic rays was of prime interest in this
595 part of the investigation, a “shear” was applied to the rotations described in this section: any AGN was displaced in
596 longitude, λ , by $\Delta\lambda = \omega \cdot \sec \phi$, where ϕ is the latitude, rather than all by the same $\Delta\lambda = \omega$, thus having the same actual
597 shift ω on the sky for each AGN, making it easy to read off the displacement of the particle. The terms “longitude”
598 and “latitude” here relate to the particular axis of rotation that is being used. (A rather similar curve, but without such
599 a large sideband noise is obtained in the case 9(b) by rotating in right ascension instead of in galactic longitude, as in
600 this region of the sky the two directions are not very different.)

601 Such a deflection of 4° by the galactic magnetic field would be quite compatible with the range of expected values
602 shown in figure 8b of Abraham et al.[1], and would correspond to a field directed “down” towards the galactic disc,
603 with a strength integrated along the particle’s path of $6\mu\text{G} \times \text{kpc}$, if the particles are protons — say, $0.3\mu\text{G}$ on average
604 over 20 kpc. The trajectory passes about 2 kpc above the galactic plane at about 7 kpc from the Galactic Centre.
605 Since deflections, at a known energy, will be proportional to nuclear charge, the particles are surely not very much
606 more highly charged than helium nuclei, and at this energy are very unlikely to be helium nuclei, as these survive
607 only about 1 Mpc in the microwave background. Of course, not having enough data to treat several different parts of
608 the sky separately, the magnetic field cannot be separated from a metagalactic field of $6\text{nG} \times \text{Mpc}$. There may well
609 be a significant metagalactic contribution seen in the widespread random $3 - 4^\circ$ scatter discussed previously, as the
610 systematic shift was only seen for a particular set of directions, at the rather low galactic latitude of 24° . The value of
611 extending these tests to a larger data set is clear.

612 A 4° displacement of the resonance of course implies some changes in the list of which AGNs appear in 3.2°
613 windows around the cosmic ray directions. With this special group of 7 cosmic ray directions there are still 2 empty
614 windows (to 75 Mpc), but the number of AGNs in the 5 active windows is increased — so it may not yet be con-

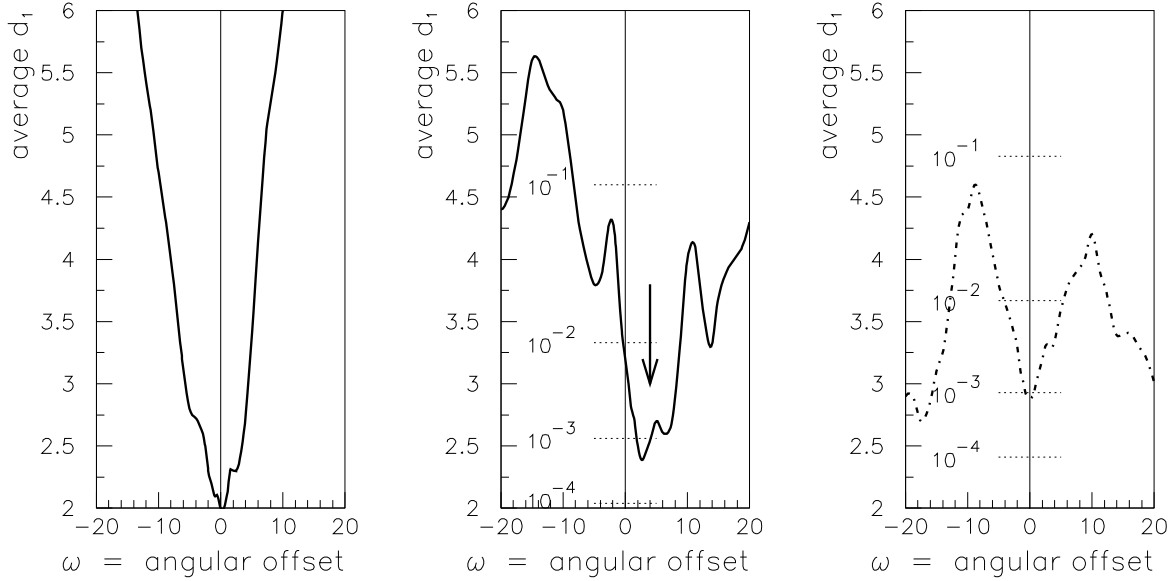


Figure 9: Position of the resonance between Auger cosmic-ray directions and the AGN positions ($z < 0.018$) when the AGN patterns are shifted in a direction ω related to galactic coordinates: in (a) and (b), the AGN positions are shifted by an angle ω parallel to the galactic plane, and in (c) by an angle ω perpendicular to the plane (see text). (a) uses the 12 cosmic-ray directions with galactic latitude, $b < -12^\circ$; (c) uses the 9 which have $b > 12^\circ$. (b) uses 7 of the latter 9, which arrive from a relatively limited part of the sky around the direction ($l = 308^\circ, b = 24^\circ$). In case (b), where the particles have passed just above the galaxy, they appear to have been deflected by about 4° , as though by a B_z component of the galactic magnetic field.

615 vincing that there must be a magnetic deflection. There now appear 9 AGNs in the standard windows around revised
 616 “undeflected” cosmic ray directions, instead of 5 in the original list. Cen A now appears in only one window rather
 617 than 2, but one of the new AGNs brought in is the FRI AGN IC 4296 on Nagar and Matulich’s list [10], which now
 618 has a distance d of 0.4° instead of 3.8° .

619 7. Correlations with AGNs in different distance ranges

620 The Auger AGN study [1] found that the correlation was most significant when only the AGNs having redshift
 621 $< z_1 = 0.018$ (distance < 75 Mpc) were used. This would have important implications, discussed in the next section.
 622 However, a maximum significance with a redshift limit of z_1 does not mean that there are few cosmic rays from
 623 beyond this limit; so direct information on the distances of travel of the detected cosmic rays should be sought. Three
 624 approaches to this tricky problem will be sketched here.

625 (1) Looking for coincidences (within 3.2°) with VCV AGNs at different distances is not helpful in a very straight-
 626 forward way, as these objects are so numerous that a typical cosmic ray direction eventually matches AGNs at different
 627 distances. This is shown in table 3, where, in the line labelled “.000-.017”, the 21 cosmic rays outside the galactic
 628 obscuration zone are shown in the sequence of their detection, with “x” showing that the particle matched an AGN in
 629 this distance range (i.e. the cosmic rays discussed previously), and “.” signifying that there was no match: there were
 630 19 “hits”. The following two lines similarly record whether these same 21 cosmic rays matched AGNs in the next
 631 succeeding ranges of redshift, each 50% as large as the first.

632
 633 The point of origin of the particle is obviously not determined unambiguously: a line of sight can pass within
 634 3.2° of more than one AGN. The selection “cuts” were chosen so as to optimize the number of hits in the first half
 635 of the run — before the dividing line in the sequences shown above — and the 10/10 hit rate in the initial period is

AGN redshift		
.000-.017:	x x x x x x x x x x x x . x x x x x x .	19
.018-.027: x x . . x . x x .	5
.028-.035:	. . . x x . x . x . x x . . x . . x x . x	10

Table 3: Sequence of cosmic rays matching AGNs (see text).

636 hence distorted. The 9/11 hit rate after this is close to what would be expected if cosmic rays do arrive from directions
637 having 3.5° rms scatter around VCV AGNs: it was found that 77% of particles should then have an AGN within
638 3.2° along the line of sight. Such simulations also show that 21 particles originating in the near zone, $z < 0.018$,
639 would typically score 12 hits in the second and third distance zones, not very different from the 15 recorded, so that
640 there are probably not very many particles originating in these more distant zones (though several associations could
641 be missed because the VCV catalogue will become significantly incomplete there). A more elaborate study of this
642 limited sample suggests that (because of the high hit-rate in the first line) most particles originated within 75 Mpc, but
643 very crudely 0-25% might come from sources beyond 75 Mpc, though a more precise estimate cannot be made.

644 (2) Resonance plots can also be used to study the extent of the correlation with increasing distance, as they are not
645 dependent on window size, though the plots are disappointing. Right ascension resonance curves for the 21 Auger
646 cosmic rays are shown in figure 10 for $\langle d_1 \rangle$ using angular distances to the nearest AGN listed in particular redshift
647 ranges of the VCV catalogue: (a) $z < 0.018$, (b) 0.018-0.027, (c) 0.028-0.036. It is at first disconcerting to see that
648 although most of the published cosmic ray directions (in unobscured regions) align closely with AGNs within 75
649 Mpc, as discussed above, and as shown in figure 10a, they also have a (much less significant) alignment with AGNs
650 between 116 and 150 Mpc (figure 10c). Although this is somewhat like the results for window hits listed above, it
651 is surprising that the 116-150 Mpc group shows a small apparent resonance near $\Delta\alpha = 0$ (that was not seen in the
652 simulated curve, below). To extract the information on distance of origin, the best that can be done at present is
653 to model the correlations one would get if the observed cosmic rays originate in a specific range of distance. So,
654 for this purpose, I have assumed that cosmic rays originate as though from any VCV AGNs, are scattered with a
655 characteristic spread, and that at greater distances a decreasing fraction of the AGN's output is seen, because GZK
656 energy losses allow us to receive only those particles emitted above an energy threshold which is increasingly above
657 57 EeV for more distant sources. The Auger sample has an energy spectrum above 57 EeV which may be represented
658 by $j = (E_{max} - E)/(E_{max} - E_o)$, where j is the fraction of particles above energy E , $E_o = 57$ EeV, and $E_{max} \approx 92$ EeV.
659 This ignores a single particle of energy well above 92 EeV, which is of no consequence in this context.

660 Assuming the local spectrum does not vary much with position in space, it might be treated roughly as though
661 E_{max} , above, is the maximum energy with which most particles are generated, and that particles cannot be received
662 here from sources more distant than D_{max} (redshift z_{max}), corresponding to the distance over which protons lose an
663 amount $\Delta \log_{10} E = 0.22$ (falling from 92 to 57 EeV). This effect is modelled approximately by multiplying the output
664 of any AGN at redshift z by a factor $(1 - (z/z_{max})^2)$ to represent the decreasing fraction of its particle output that
665 remains above 57 EeV by the time it reaches us. ("92 EeV" was quoted merely in explanation: no energy value is
666 used at this stage, but only a parameter z_{max} .)

667 Varying z_{max} (and the rms spread of cosmic rays around source AGNs) to get a crude fit to the resonance trough,
668 $\langle d_1 \rangle$ near $\Delta\alpha = 0$ in the three redshift zones out to 0.036, the best fit was with $z_{max} \approx 0.023$ and slightly favours a
669 scatter varying with \sqrt{z} (rms being 3.5° at 45 Mpc) rather than being constant. Models with $z_{max} = 0.018, 0.0216$
670 and 0.0252 gave the resonance curves shown by various thin lines in figure 10. The present rough models and low
671 statistics cannot give accurate fits, but if z_{max} is increased further the trough becomes less deep in the comparison with
672 AGNs in the nearest redshift zone, < 0.018 (figure 10(a)), that was picked out by the Auger authors. A range z_{max}
673 of 0.023 corresponds to a maximum source distance of 96 Mpc if $H_o = 72$, a travel time of close to 300 Myr. When
674 better statistics are available and refitting is attempted, the distance-dependence of the selection bias for VCV AGNs
675 should be investigated, although it would be unlikely to have much effect on a "cut-off" point.

676 (3) The alignment of cosmic rays with extended radio galaxies offers a much better chance to investigate the source
677 distances, as multiple alignments for a cosmic ray will rarely occur, apart from the special case of Cen A and NGC
678 5090. The shaded histogram in figure 11 shows the numbers of such galaxies (as listed by Nagar and Matulich) found

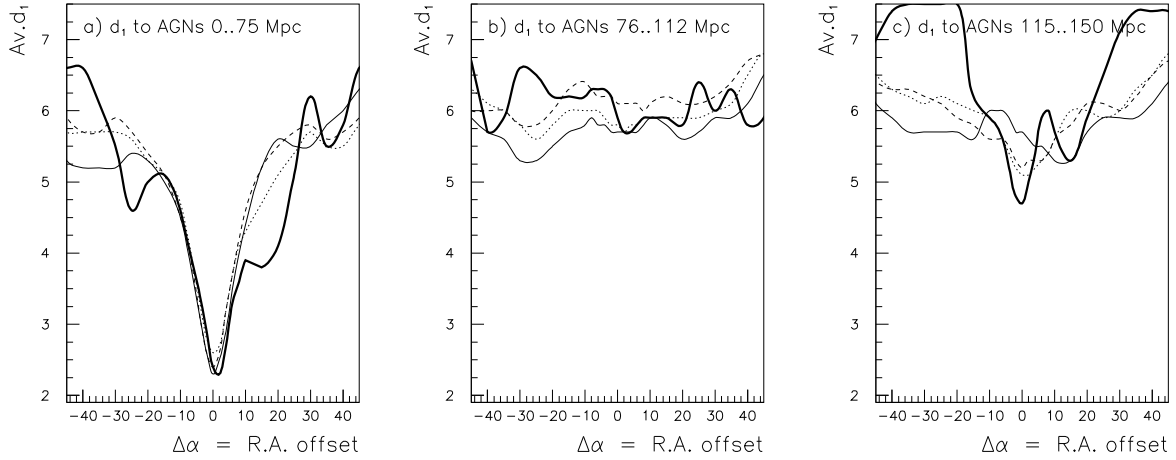


Figure 10: Right-ascension resonance plots for the 21 Auger cosmic ray directions not near the galactic plane. The mean distance to the closest VCV AGN ($\langle d_1 \rangle$) is plotted against shift $\Delta\alpha$ in right ascension of AGNs by the thick lines, (a) for AGNs in redshift range < 0.018 , (b) $0.018-0.027$, (c) $0.028-0.035$. The thinner full, dashed, dotted lines show the average curves found in models in which the cosmic rays are emitted from the vicinity of VCV AGNs, with detectable output reduced by a factor falling to zero at redshift z_{max} in the range 0.018 to 0.025 (see text). When z_{max} exceeds 0.024 , approximately, the correlation with the closer AGNs, noted by the Auger report, weakens. The seeming correlation with AGNs at $z > 0.027$ appears to stem in part from accidental alignment of AGN clusters.

679 in 20 Mpc intervals of distance, but the lightly shaded part reaching as far as 120 Mpc contains objects that seem to
 680 have been added because they were seen to align with cosmic rays, and may not be a complete sample in this region.
 681 To indicate how the radio-galaxy distribution may be expected to continue, the total number of galaxies with radio
 682 jets, listed by Liu and Zhang [20], excluding those with total jet length less than 1 kpc but without any selection based
 683 on extension of lobes seen in radio images, is shown by the line, the scale being shown on the right. Below 80 Mpc,
 684 the extended objects amount to about 40% of this total, and the scale has been chosen so that the line may thus indicate
 685 how the numbers of extended radio galaxies may be expected to continue beyond this distance. The filled circles show
 686 the numbers of cosmic rays apparently associated with the radio galaxies in each 20 Mpc — within 6° as in section 5.
 687 (The “error bars” show the effect of changing the source attribution from NGC 5090 to Cen A in 3 cases.) All these
 688 radio galaxies with jets have been included in these counts of associations, but only the extended (mostly FRI) radio
 689 galaxies mentioned by Nagar and Matulich showed an association. Thus the cosmic rays may indeed all originate
 690 within about 120 Mpc, though some sources may have been missed if the catalogue of Liu and Zhang is incomplete
 691 in the range 120-160 Mpc. The source peak near 50 Mpc is notable.

692 Hence, this treatment roughly confirms the z_{max} figure from the Auger optimization: it is probably below 120
 693 Mpc for the set of particles that still have energies above 57 EeV when they arrive. This must be controlled by their
 694 maximum energy on production, and the rate at which they lose energy.

695 8. Implications of very local sources: a cut-off in the source spectrum?

696 If one receives few or no particles above E_{thresh} which originated beyond 100 Mpc, the energy of the particles
 697 released from the source must not be too high, and the rate of loss of energy, primarily through interactions with the
 698 cosmic microwave background radiation (CMBR), must be rapid, so that the energy falls below E_{thresh} within 100
 699 Mpc. The rate of energy loss in the CMBR varies rapidly with proton energy, and it seems that the loss would be
 700 sufficient to drop below “57 EeV” within this distance only if, firstly, the particle energies are higher than quoted in the
 701 Auger paper, presumably because of remaining uncertainties in the fluorescence efficiency of air; and, secondly, the
 702 fall of the energy spectrum of cosmic rays must be steeper than that imposed by these energy losses: the observations
 703 must be closely approaching the upper energy limit of the accelerators.

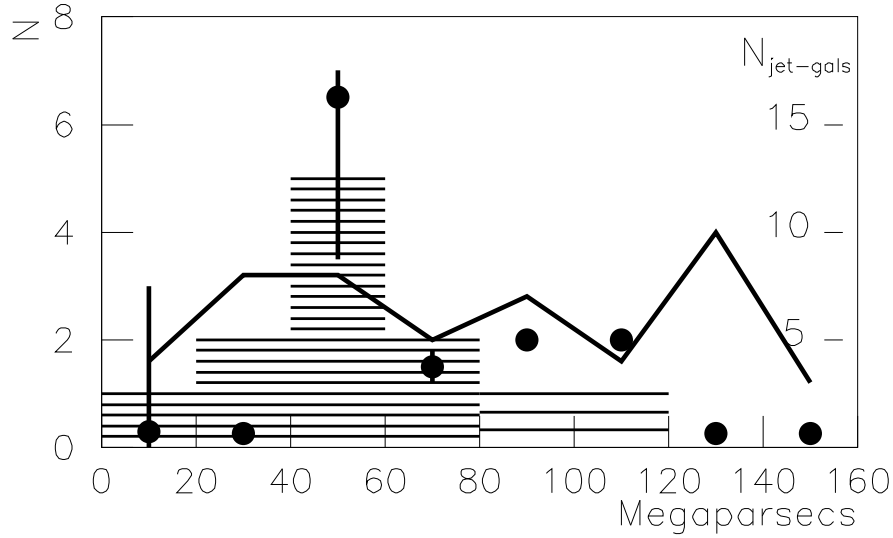


Figure 11: The histogram shows the numbers of extended radio galaxies as defined by Nagar and Matulich in 20 Mpc intervals. Beyond 75 Mpc the galaxies may have been chosen more selectively (see text). The line shows the number of galaxies with radio jets of at least 1 kpc [20] — in the field of view of the Auger Observatory, but without selection for lobe extension — the right hand scale applies to these. The black points are the numbers of cosmic rays that appear to be associated with these radio galaxies, none in fact being associated with non-extended galaxies. 3 cases attributed to NGC 5090 could alternatively be attributed to Cen A: the vertical lines show the changed counts that would result.

704 There is as yet insufficient information to resolve the interplay of several relevant factors, but the general con-
705 straints will be described with the aid of Figure 12. Consider first the lines, which trace the average change in a
706 proton’s energy with distance from its source. Ignoring the thicker lines, the steep dotted line, full line and dashed
707 line refer to protons generated with energies of 200 EeV, 100 EeV and 80 EeV respectively, and the horizontal axis
708 shows the energies on arrival if they have travelled for the distances specified on the vertical axis since leaving the
709 accelerator. (He nuclei are not considered as they photodisintegrate in ~ 1 Mpc, and larger nuclei are ignored because,
710 apart from the magnetic deflection argument given in section 6, their mean path length for serious mass loss by pho-
711 todisintegration is much less than 100 Mpc.) One expects to have a mixture of energies leaving the accelerator, with
712 a larger number starting at the lower energies. It is seen that the expected distance distribution extends far above 100
713 Mpc, in contrast with the observations.

714 The only way to remove this tail of distant sources appears to be to assume that the reported energies are too low
715 by a factor around 1.25, so that the true threshold energy is near 70 EeV. This makes the energy losses arising from
716 photopion production reactions become much more rapid. The thicker dotted, full and dashed lines again refer to the
717 proton energies after travelling various distances from the source, but assuming that the actual energies are always
718 1.25 times the figures written on the graph. The shaded area is roughly where we should expect to see the detected
719 particles, on this basis, if there are few sources within 30 Mpc (as seems to be indicated by the data) and the source
720 spectrum terminates not far from 100 EeV nominal energy (or 125 EeV on a “corrected” energy scale): there would
721 now be few particles having travelled more than 100 Mpc. This is closer to the observed distance distribution.

722 However, if we attempt to estimate the distance from the source of individual particles, by linking them to the
723 AGNs seen close to the cosmic ray arrival direction, there is a problem. In outline, one expects that the particles
724 arriving with the highest energies must have travelled a short distance, whilst the particles of lowest energy could
725 come from a wide range of distances, with different starting energies. The observed data are presented as follows.
726 The cosmic rays fairly clearly associated with extended radio galaxies (ERG) have a clear source distance, and are
727 marked with large filled circles. For those not associated with extended radio galaxies, an open circle marks the

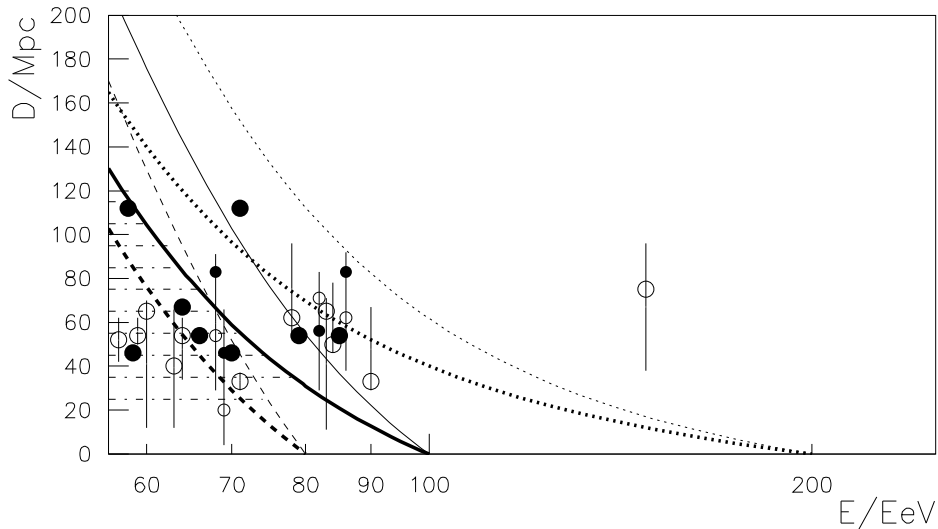


Figure 12: Distance of travel of particles arriving with different energies. For the observations, the distances are derived from redshifts of AGNs or radio-galaxies close to the line of sight (see text). The curves refer to the expected energy of protons generated with particular initial energies of 200, 100 or 80 EeV after they have travelled through the background radiation for different distances: thin lines for energies actually assigned in the Auger analysis, thick lines apply if the assigned (and plotted) energies are too low by a factor 1.25. The shaded area draws attention to the main area in which the points would be expected to lie in this latter case, assuming also that the source spectrum terminates near 100 EeV (“assigned energy”)

728 median distance of VCV AGNs within 6° and a vertical line shows the range of distances amongst this group of
 729 possible source AGNs. Where there is an adjacent extended radio galaxy and several VCV AGNs, the ERG distance
 730 and the VCV median distance are both shown, using smaller symbols (unless the ERG distance agrees with the VCV
 731 median, when the VCV indications are ignored). (There is no nearby known AGN for one of the 21 cosmic rays.)
 732 The expected correlation between energy and distance of travel is not apparent. The shape of the observed energy
 733 distribution is also a poor match, which might very possibly arise if there are event-to-event fluctuations in energy
 734 reconstruction accuracy of order 20% or more, which largely scramble the energies in such a small span of energies
 735 as is represented here — and reminiscent of the Haverah Park example discussed in section 4. A larger data sample
 736 is needed to make more of this energy spectrum, to find out just how steeply it must fall at this apparent termination.
 737 Simulations of energy propagation have been made but will be published separately.

738 9. Summary: conclusions concerning the cosmic-ray sources

739 The report [1] by the Auger collaboration, that most of the cosmic rays that had been detected above an energy
 740 of 57 EeV came from directions within 3.2° of an optically detected AGN within about 75 Mpc, listed in the 12th
 741 catalogue of Véron-Cetty and Véron, marked the first instance of a fine-scale anisotropy seen in charged-particle
 742 astronomy. It was shown in section 2 that cosmic rays appeared to come from regions where AGNs were clustered.
 743 Sky distributions on different scales are consistent with the cosmic rays originating from sources in or near such
 744 AGNs, typically Seyfert galaxies, and being deflected randomly by $3 - 4^\circ$ on their way to us. As this scattering angle
 745 is similar to the separation of AGNs in the source region, it will not usually be clear what object is the actual source.
 746 The appearance of some very weak objects closest to the observed direction is hence not significant. In section 3, a
 747 uniform-exposure polar plot was recommended for displaying quantitative aspects of the distribution of cosmic rays
 748 and possible source objects such as AGNs on the sky, and the distribution of cosmic rays was seen to follow the
 749 distribution of the VCV AGNs on the large scale, with about 0.1 cosmic rays detected during the reported observing
 750 run per catalogued AGN within 75 Mpc, where the exposure efficiency was high.

751 A method of showing the close correlation with directions of AGNs or other objects that did not require choice
 752 of a particular correlation “window” size was introduced in section 4 — a “right ascension resonance” in average

753 closest distance — which showed the rapidity of decoherence of these patterns on the sky when they were displaced
754 slightly. This showed the cross-correlation in a very immediate way, that could be used to explore related associations
755 in other regions. As this did not make use of any specially optimized window radius, it could be used to check the
756 very high statistical significance of the correlation with AGNs. The association of cosmic rays with the extended radio
757 galaxies with radio jets within 120 Mpc (Nagar and Matulich [10]), most of which were not in the VCV optically-
758 based catalogue, was, quite separately, significant at around the 1 in 10^6 level, with an average of around 1 detected
759 cosmic ray per object, although not all seem to be active at the present time: the nearby and spectacular low-energy
760 electron accelerators Cen A and Fornax A are probably currently switched off at these ultra high energies (otherwise
761 the former would have completely outshone the other FRI radio galaxies, because of its proximity, as it does in the
762 case of low-energy synchrotron radiation).

763 If the few brightest radio galaxies within ~ 80 Mpc, notably M87 (Virgo A), Cen A and Fornax A, had been the
764 dominant sources, their output must have been spread widely over the sky by magnetic deflections [4, 5, 6]. How-
765 ever, only a small proportion of such widely-scattered cosmic rays would line up within 3.2° of a catalogued AGN,
766 as pointed out in section 3: this is not the case. If, on the other hand, the lines-of-sight to cosmic ray sources are
767 scattered around many VCV AGNs by $3 - 4^\circ$, most of the cosmic ray distributions are well described. In summary,
768 the small apparent scale of $3-4^\circ$ for the spread of cosmic ray directions around source regions indicates that there are
769 many more sources than there are strong radio-emitting AGNs. So although perhaps 40% of the detected cosmic rays
770 in this energy region appear to come from FRI or similar radio galaxies at typical distances near 50 Mpc, the remain-
771 der presumably come from numerous weaker sources, which reside in these AGN clusters, and accelerate protons to
772 very similar maximum energies. Ghisellini et al [16] have also emphasised the possibility that any objects that reside
773 in galaxy clusters are candidates, and have shown that cosmic-ray directions correlate with the density of ordinary
774 galaxies. It is not known whether the pattern de-coheres with galaxy density as rapidly as with AGNs, but it seems
775 likely that AGNs do trace galaxy density. Although these authors particularly draw attention to the possibility that
776 magnetars might be the sources [17], the very significant appearance of FRI radio galaxies close to the directions from
777 which cosmic rays arrive makes it appear more probable that the Seyfert galaxies are indeed the currently less-active
778 end of a distribution of jet-related sources of cosmic rays of $(0.7 - 1.2) \times 10^{20}$ eV. (Only 25% of the VCV AGNs are
779 not known radio emitters.) As it is apparently the case that the particles, which, it is argued, are largely protons at
780 the very highest energies, can rarely reach us from more than 100 Mpc away, it appears that the true energies must
781 be around 25% higher than currently estimated by the Auger methods, and that the accelerator output probably drops
782 rather sharply in the region of 1.2×10^{20} eV. It is, however, surprising that this assembly of stronger and weaker
783 sources produces a total spectrum with a sharp cut-off.

784
785 *Postscript* Although further Auger observations have not yet been published, talks (e.g. [22]) indicate that a later
786 exposure has given a very different sky distribution, without the same concentration near AGNs. As was shown above,
787 the published data show correlations with AGNs and related objects that are not accidental; but the success of a 57
788 EeV threshold, for example, in extracting the vital proton component that can point back to sources may not be robust,
789 as seen in the comparison of sky maps from three experiments at the end of section 4. The success of the initial phase
790 might even, for instance, have depended on the presence of excessive fluctuations in (proton) energy reconstruction,
791 occurring in somewhat smaller fields of less well-behaved detectors, that falsely promoted the energies of some pro-
792 tons! It seems that the recognition of proton-induced showers will be an important task. The appearance of very
793 widely-scattered cosmic ray directions near the maximum energies gives support to the indication from the Auger
794 studies on depth of shower maximum [21] that a heavy-nucleus component becomes very important as the extreme
795 energies are approached.

796 *Acknowledgements*

797
798 I wish to thank Ralph Engel for stimulating me to offer suggestions on the Auger directions, both Alan Watson
799 and Johannes Knapp for several critical and perceptive discussions and much encouragement, information and help,
800 Jeremy Lloyd Evans and Jim Hinton for useful suggestions, and Mansukh Patel and Ronald Bruijn for further help.
801

802 **References**

- 803 [1] The Pierre Auger Collaboration: J. Abraham et al., (2008) *Astroparticle Physics* 29: 188-204; and
804 (2007) arXiv (astro-ph) 0712.2843 v1.
805 [2] R U Abbasi et al. (2005), *Astrophys. J.* 622, 910
806 [3] M-P Véron-Cetty and P Véron: *Astron. Astrophys.* 455 (2006) 773:
807 accessed via <http://vizier.u.strasbg.fr/viz-bin/VizieR> .
808 [4] P L Biermann et al. (2008), arXiv:0811.1848v3 [astro-ph]
809 [5] P L Biermann (2008), lectures at 400th Heraeus Seminar
810 <http://www-ik.fzk.de/ik/Heraeus400/talks/15-Biermann.pdf>
811 [6] D S Gorbunov, Tinyakov P G, Tkachev I I and Troitsky S V (2008): arXiv:0804.1088v1 [astro-ph].
812 [7] M R George, Fabian A C, Baumgartner W H Mushotzky R F and Tueller J (2008), *MNRAS* . arXiv:0805.2053v1 [astro-ph].
813 [8] I V Moskalenko, Stawarz I, Porter T A and Cheung C C (2008) *subm. Astrophys. J.*, and arXiv:0805.1260v1 [astro-ph]
814 [9] A M Hillas (1984) *Ann. Revs. Astron. Astrophys.* 22: 425
815 [10] N M Nagar and Matulich J (2008) *subm. Astron. Astrophys.*; and arXiv:0806.3220v1 [astro-ph].
816 [11] Ingyin Zaw, Farrar Glennys R and Greene Jenny E (2008): arXiv:0806.3470v1 [astro-ph]
817 [12] T Stanev (2008) lecture at 400th Heraeus Seminar
818 <http://www-ik.fzk.de/ik/Heraeus400/talks/07-Stanev-Intro.pdf>
819 [13] R U Abassi et al.: The High Resolution Fly's Eye Collaboration (2008) *Astroparticle Physics* 30: 175-9.
820 [14] web-site http://physics.rutgers.edu/~lsct/agn/high_e_events.txt
821 [15] S Westerhoff et al. *Nucl. Phys. B (Proc. Suppl.)* 136 (2004) 46-51
822 [16] G Ghisellini, Ghirlanda G, Tavecchio F, Fraternali F and Pareschi G (2008): *MNRAS* ; arXiv:0806.2393v1 [astro-ph].
823 [17] J Arons (2003) *Astrophys. J.* 589: 871
824 [18] G Cunningham et al. (1980) *Ap.J. Letters* 236: L71
825 [19] Y Uchihori et al. (2000), *Astroparticle Phys* 13: 155.
826 [20] F K Liu and Zhang Y H (2002) *Astron. Astrophys.* 381: 757-60.
827 List only available electronically: <http://cdsweb.u-strasbg.fr/cgi-bin/qcat?J/A+A/381/757>
828 [21] M Unger for the Pierre Auger Collaboration (2007), 30th International Cosmic Ray Conference, Merida, Vol 4 (HE part 1) p 373
829 [22] APS 2009: http://blogs.nature.com/news/blog/2009/05/aps_2009_pierre_auger_backs_of.html

830 **A. AGN counts in Véron-Cetty Véron 12th edition catalogue**

831 Figure 13 shows the number of objects listed in the southern hemisphere (declination $< +15^\circ$) per Mpc of distance,
832 D , converting from redshift to distance using a value $H_0 = 72 \text{ km s}^{-1} \text{ Mpc}^{-1}$ for Hubble's constant. The lines refer to
833 objects in different ranges of absolute magnitude ("−19" indicating −19.0 to −19.9, for example).

834 The lines −20, −21 and −22 suggest a trend $dn/dD \propto D$ initially, as though the objects are distributed in a slab whose
835 thickness is a few Mpc, but then falling sharply below this trend as though there is a limiting apparent magnitude
836 for efficient detection. Thus objects with absolute magnitude brighter than −20.0 would be recorded inefficiently
837 at distances beyond the 75 Mpc limit of the Auger sample. The median absolute magnitude for the most closely
838 associated AGNs at the closer distances appears to be about −19.0, so beyond 75 Mpc, the catalogue would fail to list
839 many of any truly associated AGNs (as remarked in [1], and one would need large statistics to map out the sources
840 beyond there. If the number of listed AGNs within 75 Mpc had been much greater, the probability of associations
841 within 3.2° with any arbitrary direction would have been large, nullifying the signal.

842 **B. Array exposure to different celestial directions: equal-exposure plot radius.**

The effective detection area presented to a source at zenith angle θ is $A \cdot \cos \theta$ if the detecting area on the ground
always has a fixed value A . Let λ be the magnitude of the observatory's latitude (i.e. always treated as positive). For
a source at polar angle p , its zenith angle varies during the sidereal day according to the expression

$$\cos \theta = \cos p \cdot \sin \lambda + \sin p \cdot \cos \lambda \cdot \cos H \quad (2)$$

where H is the hour angle relative to the source's right ascension, which increases uniformly with time, from 0 when
 θ is least (source highest in the sky), to 360° after a complete sidereal day. Thus the time average of the effective
detecting area is

$$\langle A \cdot \cos \theta \rangle = A \int \cos \theta \cdot dH / 360^\circ \quad (3)$$

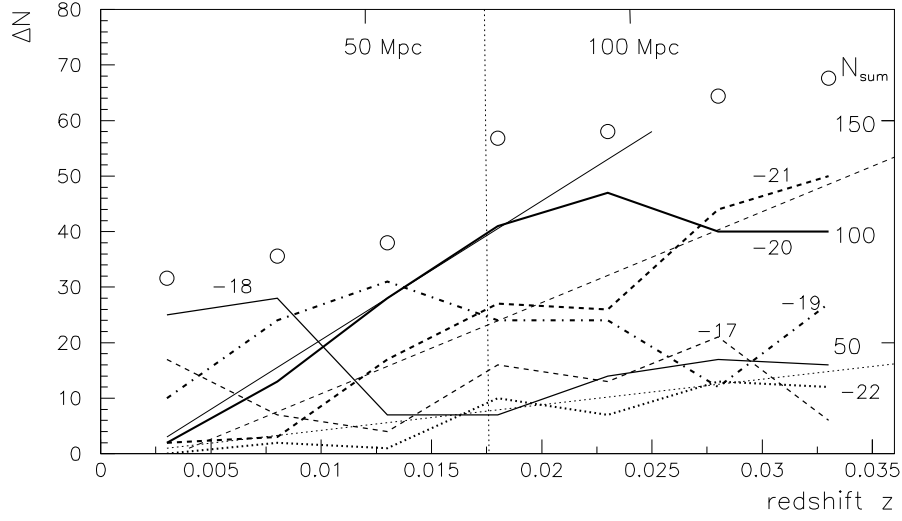


Figure 13: Distribution in distance of AGNs (declination $< +15^\circ$) in VCV catalogue. Lines marked -17 ... -21 refer to AGNs having absolute magnitude -17.0 to -17.9, -18.0 to -18.9...-21.0 to -21.9. Line -22 refers to all magnitudes brighter than -22.0 (though only 27% of those included are brighter than -22.9). For the three brighter groups, a dotted line shows the straight-line trend. Open circles show totals (scale on right).

843 where the integral is taken over all values of H (here expressed in degrees) which give $\theta < \theta_{max}$. For the Auger array,
 844 $\theta_{max} = 60^\circ$ and $\lambda = 35.2^\circ$. At polar angles greater than $(90^\circ + \theta_{max} - \lambda)$ sources never rise to zenith angles less than
 845 θ_{max} : this limit is 114.8° for the Auger observatory, meaning that sources with declinations above $+24.8^\circ$ are never
 846 recorded. Where $\theta_{max} > 90^\circ - \lambda$, as at Auger, some (“circumpolar”) sources never fall further from the zenith than
 847 θ_{max} : they have $p < \theta_{max} - (90^\circ - \lambda)$ and are detectable all day. If $\theta_{max} \leq 90^\circ - \lambda$, though, sources closer to the pole
 848 than $p' = 90^\circ - \theta_{max} - \lambda$ are never recorded (and on an equal-exposure plot, this range $0..p'$ is contracted to a point
 849 at the centre of the plot). To find the effective detecting area for a source at any selected polar angle p , the integral in
 850 equation 3 is evaluated over the range of H for which θ is less than θ_{max} , noting that for some values of p this condition
 851 is always or never satisfied, as just mentioned.

Having determined the efficiency of the detector for sources of each polar angle, as just described, the radius R at which a source should be shown in an equal-exposure plot is

$$R(p) = k \sqrt{\int_{z=0}^{z=p} \langle A \cos \theta \rangle \sin z \cdot dz}, \quad (4)$$

852 where the variable z refers to a polar angle, and $\langle A \cos \theta \rangle$ is a function of this polar angle, from equations 3 and 2.
 853 The limit of integration, p , is the polar angle at which R is required. k is chosen to make $R \rightarrow 1$ at large p . Table 4
 854 tabulates the calculated efficiency and polar-plot radius, R , at intervals of 2° in polar angle. The numerical results can
 855 be represented to a reasonable approximation by the following formula:

For the Pierre Auger Observatory,

$$R = [1 + 0.27 \exp(-p/5.7^\circ)] \cdot \sin(0.746p), \quad (p \text{ in degrees}) \quad (5)$$

856 with the maximum divergence from the tabulated value being 0.006. However, if the term in square brackets is
 857 removed, leaving just the sine, the error is only significantly increased at polar angles $< 16^\circ$, reaching 0.012 at 8° ,
 858 and as few cosmic rays are detected so close to the pole, this small distortion in their plotted density is probably
 859 immaterial. This formula should not be used for polar angles beyond the theoretical maximum of 114.8° .

860 To plot a cosmic-ray direction, or an astronomical object, at right ascension α and declination δ , the polar distance
 861 is calculated ($p = 90^\circ - \delta$ for a northern hemisphere plot, or $p = 90^\circ + \delta$ for the southern hemisphere), then R is

862 found by interpolation in the table or by use of approximation given in equation (5). The coordinates on the plot are
 863 then $x = R \cdot \cos \alpha$, $y = R \cdot \sin \alpha$.

p	Efficiency	R	p	Efficiency	R
0	0.576	0.000	60	0.331	0.702
2	0.576	0.030	62	0.325	0.720
4	0.575	0.061	64	0.319	0.739
6	0.489	0.090	66	0.312	0.756
8	0.436	0.115	68	0.305	0.774
10	0.413	0.140	70	0.298	0.791
12	0.401	0.163	72	0.290	0.807
14	0.394	0.187	74	0.282	0.822
16	0.389	0.211	76	0.274	0.837
18	0.387	0.234	78	0.265	0.852
20	0.385	0.258	80	0.256	0.866
22	0.383	0.282	82	0.246	0.879
24	0.382	0.306	84	0.237	0.892
26	0.381	0.329	86	0.227	0.904
28	0.380	0.353	88	0.216	0.915
30	0.379	0.376	90	0.206	0.926
32	0.378	0.400	92	0.195	0.936
34	0.377	0.423	94	0.183	0.945
36	0.375	0.446	96	0.172	0.954
38	0.373	0.469	98	0.160	0.962
40	0.371	0.492	100	0.147	0.969
42	0.369	0.514	102	0.135	0.976
44	0.366	0.536	104	0.121	0.981
46	0.363	0.558	106	0.107	0.987
48	0.359	0.580	108	0.092	0.991
50	0.356	0.601	110	0.075	0.995
52	0.351	0.622	112	0.056	0.998
54	0.347	0.643	114	0.029	1.000
56	0.342	0.663	116	0.000	1.000
58	0.337	0.682			

Table 4: Detection efficiency and radial position R in equal-exposure polar plot for the Auger Observatory.